Spatial mapping of key plant functional traits in terrestrial ecosystems across China

Nannan An[1,2,3], Nan Lu[2,3], Weiliang Chen[2], Yongzhe Chen[2,4], Hao Shi[2,3], Fuzhong Wu[1], Bojie Fu[2,3]

[1]Key Laboratory of Humid Subtropical Eco-geographical Process of Ministry of Education, School of Geographical Sciences, Fujian Normal University, Fuzhou 350117, PR China

[2]State Key Laboratory of Urban and Regional Ecology, Research Center for Eco-Environmental Sciences, Chinese Academy of Sciences, Beijing 100085, PR China

[3]University of Chinese Academy of Sciences, Beijing 101408, PR China

[4]Department of Geography, The University of Hong Kong, Hongkong, 999077, PR China

Correspondence to: Nan Lu (nanlv@rcees.ac.cn)

Abstract

Trait-based approaches are of increasing concern in predicting vegetation changes and linking ecosystem structures to functions at large scales. However, a critical challenge for such approaches is acquiring spatially continuous plant functional trait maps. Here, six key plant functional traits were selected as they can reflect plant resource acquisition strategies and ecosystem functions, including specific leaf area (SLA), leaf dry matter content (LDMC), leaf N concentration (LNC), leaf P concentration (LPC), leaf area (LA) and wood density (WD). A total of 34589 in-situ trait measurements of 3447 seed plant species were collected from 1430 sampling sites in China and were used to generate spatial plant functional trait maps (~1 km), together with environmental variables and vegetation indices based on two machine learning models (random forest and boosted regression trees). To obtain the optimal estimates, a weighted average algorithm was further applied to merge the predictions of the two models to derive the final spatial plant functional trait maps. The models showed a good accuracy in estimating WD, LPC and SLA, with average R^2 values ranging from 0.48 to 0.68. In contrast, both the models had weak performance in estimating LDMC, with average R^2 values less than 0.30. Meanwhile, LA showed considerable differences between the two models in some regions. Climatic effects were more important than those of edaphic factors in predicting the spatial distributions of plant functional traits. Estimates of plant functional traits in the northeast China and the Qinghai-Tibet Plateau had relatively high uncertainties due to sparse samplings, implying a need of more observations in these regions in the future. Our spatial trait maps could provide critical support for trait-based vegetation models and allow exploration into the relationships between vegetation characteristics and ecosystem functions at large scales. The six plant functional trait maps for China with 1 km spatial resolution are now available at https://figshare.com/s/c527c12d310cb8156ed2 (An et al., 2023).

1 Introduction

Climate change has been affecting vegetation distributions and biogeochemical cycling globally and altering their feedbacks to the climate system (Kirilenko et al., 2000; Finzi et al., 2011; Jónsdóttir et al., 2022). Dynamic global vegetation models (DGVMs) are powerful tools for predicting changes in vegetation and ecosystem-atmosphere exchanges (e.g., water, carbon and nutrient cycling) in a changing climate (Foley et al., 1996; Peng, 2000). However, conventional DGVMs are still insufficient realistic, largely due to their dependence on the plant functional types (PFTs) assumption (Sitch et al., 2008; Yurova and Volodin, 2011; Scheiter et al., 2013). PFTs in conventional DGVMs commonly have fixed attributes (mostly trait values) (van Bodegom et al., 2012; Wullschleger et al., 2014) that do not reflect plant adaptation to environments, limiting the quantification of carbon-water-nutrient feedbacks between terrestrial ecosystems and the atmosphere (Zaehle and Friend, 2010; Liu and Yin, 2013). Trait-based approaches can provide a robust theoretical basis for developing the next generation of DGVMs (van Bodegom et al., 2012; Sakschewski et al., 2015; Matheny et al., 2017). Plant functional traits, which are closely associated with ecosystem functions (Diaz et al., 2004; Yan et al., 2023), can effectively reflect response and adaptation of plants to environmental conditions (Myers-Smith et al., 2019; Qiao et al., 2023).

Attempts to predict spatially continuous trait maps have been conducted at regional to global scales (e.g., Madani et al., 2018; Moreno-Martínez et al., 2018; Boonman et al., 2020; Loozen et al., 2020; Dong et al., 2023). Webb et al. (2010) proposed that the environment creates a filtered trait distribution along an environmental gradient, and such trait-environment relationships offer fundamental support to predict the spatial distributions of plant functional traits through extrapolating local trait measurements. Boonman et al. (2020) mapped the global patterns of specific leaf area (SLA), leaf N concentration (LNC) and wood density (WD) based on a set of climate and soil variables. As the number of available regional and global trait databases increases (Wang et al., 2018; Kattge et al., 2020), trait-environment relationships are becoming increasingly quantitative and accurate (Bruelheide et al., 2018; Myers-Smith et al., 2019). Alternatively, remote sensing approaches, such as empirical methods and physical radiative transfer models (e.g., partial least squares regression and PROSPECT model), have been developed to estimate plant physiological, morphological and chemical traits (e.g., leaf chlorophyll content, SLA, LNC and leaf dry matter content (LDMC)) (Darvishzadeh et al., 2008; Romero et al., 2012; Ali et al., 2016). Vegetation indices, such as normalized difference vegetation index and enhanced vegetation index (EVI), have been successful in estimating plant functional traits of croplands, grasslands and forests (Clevers and Gitelson, 2013; Li et al., 2018; Loozen et al., 2018). Loozen et al. (2020) demonstrated that EVI was the most important predictor for mapping the spatial pattern of canopy nitrogen in European forests. Admittedly, a recent study has suggested that combining environmental variables and vegetation indices can improve the predictive accuracy of canopy nitrogen compared to those based on vegetation indices alone (Loozen et al., 2020).

Although there have been reports on plant functional trait distributions in China in some global or regional researches (e.g., Yang et al., 2016; Butler et al., 2017; Madani et al., 2018; Moreno-Martínez et al., 2018; Boonman et al., 2020), there are still large uncertainties in characterizing the spatial distributions of plant functional traits in China. First, global studies generally have relatively few and unevenly distributed sampling sites across China (Butler et al., 2017; Madani et al., 2018; Boonman et al., 2020), impeding our understanding of the true spatial characteristics of trait variability. Second, the spatial patterns of traits among these studies are usually inconsistent. For example, Moreno-Martínez et al. (2018) and Madani et al. (2018) demonstrated that SLA values were low in the southeast areas but high in the southwest areas of China, whereas Boonman et al. (2020) found the opposite. Third, most studies focused on leaf traits (Yang et al., 2016; Loozen et al., 2018; Moreno-Martínez et al., 2018), whereas traits associated with the whole-plant strategies, such as WD, were ignored. Therefore, mapping and verifying the spatial patterns of key functional traits that reflect the whole plant economics spectrum in China is a top priority.

In this study, our main objective was to generate spatial maps for several key plant functional traits, through combining field measurements, environmental variables and vegetation indices. We selected six plant functional traits including SLA, LDMC, LNC, LPC, LA and WD. As key leaf economics traits, SLA, LDMC, LNC and LPC were selected because they are closely linked to plant growth rate, resource acquisition and ecosystem functions (Wright et al., 2004; Diaz et al., 2016). LA is indicative of the trade-off between carbon assimilation and water-use efficiency (Wright et al., 2017), and WD reflects the trade-off between plant growth rate and support cost, with a higher WD linked to a lower growth rate, a higher survival rate and a higher biomass support cost (King et al., 2006). For each plant functional trait, we predicted spatial pattern at a 1 km resolution using an ensemble modelling algorithm based on two machine learning methods (i.e., random forest and boosted regression trees).

2 Materials and Methods

2.1 Overview

The spatial maps of plant functional traits in China were generated based on machine learning methods trained by a large dataset of in-situ field measurements, environmental variables and vegetation indices in three steps (Fig. 1). First, in-situ field measurements of six plant functional traits were collected from TRY and China databases as well as published literature, and the PFTs of plant species were classified based on plant growth form, leaf type and leaf phenology. Multiple gridded predictors of climate, soil, topography and vegetation indices were used after avoiding the collinearity among them. Second, random forest and boosted regression trees were used to train the relationships between plant functional traits and predictors for each PFT individually. Third, the spatial abundance of each PFT within 1 km grid cell was calculated using land cover map (100 m). Community-weighted trait value within 1 km grid cell was calculated based on the abundance of each PFT and their predicted trait values in Step 2. To reduce the variability of different single-models, we derived the final spatial maps of plant functional traits using an ensemble model algorithm to merge the predictions of random forest and boosted regression trees according to their cross-validated R^2 values.

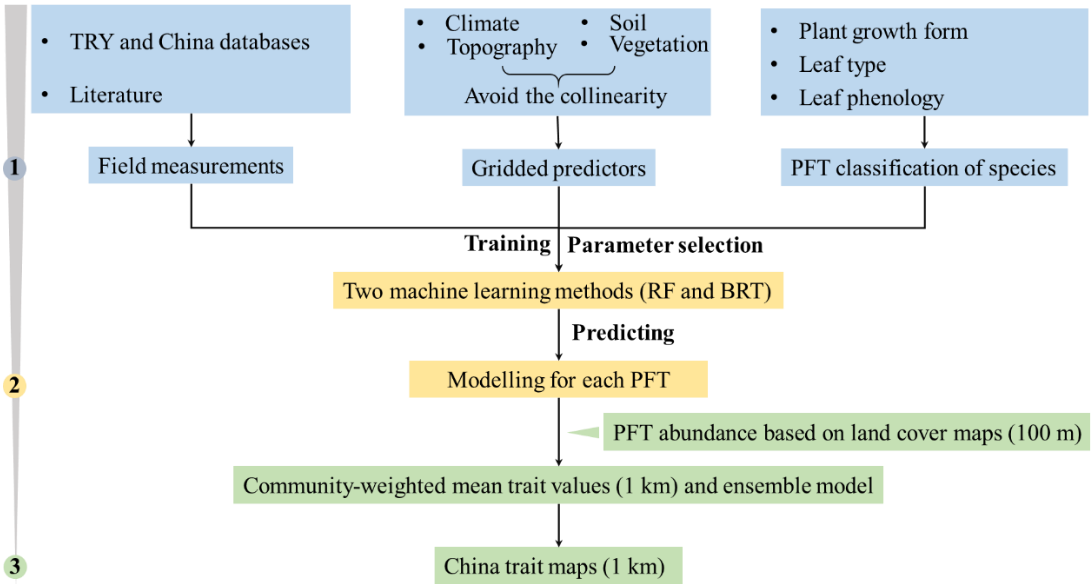

Figure 1. Methodological workflow for spatial mapping of plant functional traits. Trait mapping is performed in three steps. Step 1: in-situ field measurements of plant functional traits, PFT classification of plant species and gridded predictors were collected. Step 2: two machine learning methods were used to predict trait values by training field measurements and predictors for each PFT. Step 3: spatialization of trait maps by calculating the abundance of each PFT using 100 m land cover map and predicted trait values within 1 km grid cell. PFT, plant functional type; RF, random forest; BRT, boosted regression trees.

2.2 Plant functional trait collection and data processing

The information on the six plant functional traits and their ecological meanings are described in Table 1. Plant trait data was obtained and collected via two main sources. The first source was public trait databases, including the TRY database (Kattge et al., 2020) and the China Plant Trait Database (Wang et al., 2018). The second source was from literature (listed in Appendix A). To ensure data quality and comparability, we only included trait observations that met the following five criteria: 1) Measurements must be obtained from natural terrestrial fields in order to minimize the influence of management disturbance, and observations from croplands, aquatic habitats, control experiments and gardens were excluded; 2) According to the mass ratio hypothesis, the effect of plant species on ecosystem functioning is determined to an overwhelming extent by the traits and functional diversity of the dominant species and is relatively insensitive to the richness of subordinate species (Grime, 1998). Thus, we only included studies that measured plant trait observations from all species or dominant species within a community; 3) In order to consider the intraspecific trait variation, when the same species occurred at the same sampling site from different studies, we included all original observed data from different studies rather than averaging the values at the species level (Jung et al., 2010; Siefert et al., 2015); 4) Plant trait observations must be made on mature and healthy plant individuals, so some specific growth stages (e.g., seedling) and size classes (e.g., sapling) were excluded to reduce the confounding effect of ontogeny (Thomas, 2010); 5) We only included studies with clear geographical coordinates to match predictor variables. The sampling location and sampling time were also included in the dataset. The sampling time mostly focused on the growing season of a year (i.e., May-October), which can ensure the relative consistency of sampling time to minimize the effects of seasonality. Plant functional traits must be sampled and measured according to standardized measurement procedures (Perez-Harguindeguy et al., 2013) to reduce the variation and uncertainty among different data sources. In this study, we included SLA measurements on sun-leaves, and WD measurements on main stem of woody species.

Table 1 Description of plant functional traits selected in this study and their relevant ecosystem functions.

Trait	Abbreviation	Description	Relevant ecosystem functions
Specific leaf area	SLA	As a core leaf economics trait (Wright et al., 2004), it is related to trade-off between leaf lifespan and carbon acquisition as well as light competition (Reich et al., 1991)	Productivity, litter decomposition, competitive ability (Bakker et al., 2011; Smart et al., 2017)
Leaf dry matter content	LDMC	Strongly related to resource availability and potential growth rate (Hodgson et al., 2011)	Productivity, litter decomposition, herbivore resistance and drought tolerance (Bakker et al., 2011; Smart et al., 2017; Blumenthal et al., 2020)
Leaf N concentration	LNC	As a core leaf economics trait, it is strongly related to photosynthetic capacity (Wright et al., 2004)	Productivity, nutrient cycling, litter decomposition (LeBauer and Treseder, 2008; Bakker et al., 2011)
Leaf P concentration	LPC	As a core leaf economics trait, it is strongly related to photosynthetic capacity (Wright et al., 2004)	Productivity, nutrient cycling, litter decomposition (LeBauer and Treseder, 2008; Bakker et al., 2011)
Leaf area	LA	Trade-off between carbon assimilation and water use efficiency, it is related to energy balance (Wright et al., 2017)	Productivity (Li et al., 2020)
Wood density	WD	A measure of carbon investment, representing the trade-off between growth and mechanical support (Martínez-Vilalta et al., 2010)	Drought tolerance, productivity (Hoeber et al., 2014; Liang et al., 2021)

The plant trait data was checked for possible errors and corrected in three steps as follows. First, species name and taxonomic nomenclature were corrected and standardized according to the Plant List (http://www.theplantlist.org/) using the ‘plantlist’ package. Second, illogical values, repeated values and outliers were removed, which were defined by observations exceeding 1.5 standard deviations from the mean trait value for a given species (Kattge et al., 2011). Third, we appended information on plant growth form, leaf type and leaf phenology from the TRY categorical traits database (https://www.try-db.org/TryWeb/Data.php#3) and *Flora Reipublicae Popularis Sinicae* (http://www.iplant.cn/frps), which were used to match species names to PFTs. We associated each species with a corresponding PFT based on plant growth form (tree, shrub and grass), leaf type (broadleaf and needleleaf) and leaf phenology (evergreen and deciduous). For example, the information on *Salix matsudana* is: tree, deciduous and broadleaf, thus, we were able to associate the PFT of deciduous broadleaf forest (DBF) to this species. The species that did not correspond to any PFT were discarded. After these treatments, we collected a total of 34589 trait measurements from 1430 sampling sites for our database, representing 3447 species from 195 families and 1066 genera (Fig. 2). Information on the statistics for the six plant functional traits collected in this study is shown in Table B1 in Appendix B.

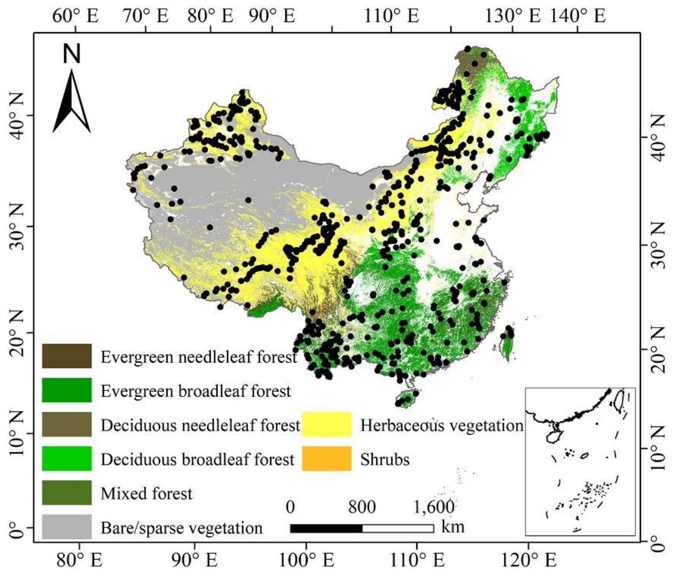

Figure 2. The spatial distribution of sample sites across different ecosystems in China. The white areas represent artificial land cover types.

2.3 Preparing predictor variables

2.3.1 Climate data

Twenty-one climate variables were used in this study, including 19 bioclimate variables, solar radiation (RAD) and aridity index (AI) (Table B2 in Appendix B). The 19 bioclimate variables and RAD were obtained from WorldClim version 2.1 for the period from 1970 to 2000 (https://www.worldclim.org/data/worldclim21.html). The AI data was extracted from the CGIAR Consortium of Spatial Information (CGIAR-CSI) for the period from 1970 to 2000 (http://www.csi.cgiar.org) (Trabucco and Zomer, 2018). The spatial resolution of climate data is 1 km.

2.3.2 Soil data

Twelve soil variables were included in this study, representing different aspects of soil properties, i.e., soil texture, bulk density (BD), pH and soil nutrients (Table B2 in Appendix B). All soil variables were extracted from the Soil Database of China for Land Surface Modeling (http://globalchange.bnu.edu.cn/research/soil2) (Shangguan et al., 2013). Given the importance of topsoil properties on community composition (Bohner, 2005), we averaged the first four layers to represent the topsoil properties (~ 30 cm) in our study. The spatial resolution is 1 km.

2.3.3 Topography

The topographic variable was elevation. Elevation data was extracted from the STRM 90m dataset in China based on the SRTM V4.1 database (https://www.resdc.cn/data.aspx?DATAID=123). The spatial resolution is 1 km.

Given the collinearity among climate and soil variables, we reduced the dimensionality of these predictors based on Pearson's correlation coefficient (r) (Figs. B1 and B2 in Appendix B). Among a set of highly correlated variables ($r > 0.75$), only one variable was retained in subsequent analysis to ensure a combination of different environmental variables. The final selection of environment predictors included twenty variables: mean annual temperature (MAT), mean diurnal range (MDR), min temperature of the coldest quarter (Tmin), max temperature of the warmest quarter (Tmax), temperature seasonality (TS), mean annual precipitation (MAP), precipitation seasonality (PS), precipitation of the wettest quarter (PEQ), precipitation of the driest quarter (PDQ), AI, RAD, elevation, soil sand content (SAND), pH, BD, soil total N (STN), soil total P (STP), soil available P (SAP), soil alkali-hydrolysable N (SAN) and cation exchange capacity (CEC).

2.3.4 Vegetation indices

Three categories of vegetation indices were included in this study (Table B2 in Appendix B). First, EVI was extracted from the MOD13A3 V006 product (https://lpdaac.usgs.gov/products/mod13a3v006/). This product is available as a monthly average with the spatial resolution of 1 km, ranging from January 2000 to December 2018. Second, MODIS reflectance data was also extracted from the MOD13A3 V006 product, including MIR reflectance, NIR reflectance, red reflectance and blue reflectance. Third, the MERIS terrestrial chlorophyll index (MTCI) was extracted from the Natural Environment Research Council Earth Observation Data Centre (NERC-NEODC, 2005) (https://data.ceda.ac.uk/). MTCI data is available globally as a monthly average at 4.63 km spatial resolution, and ranges from June 2002 to December 2011. It is noted that valid MTCI values should be greater than 1, so our study deleted any values less than 1.

To avoid collinearity, we also reduced the dimensionality of vegetation indices based on r values (Fig. B3 in Appendix B). Most selected variables were related to growing season due that plant functional traits were measured during the growing season. Furthermore, based on the results of Pearson's correlation analysis, MTCI, MIR, NIR, red and blue in January showed low correlations with those in growing season, thus they were included in subsequent analysis. The final selection included 36 variables: annual EVI, monthly EVI (May, June, July, August and September), monthly MTCI, MIR, NIR, red and blue (all for January, June, July, August and September).

Both environmental variables and vegetation indices were resampled to a consistent spatial resolution of 1 km using the nearest neighborhood method.

PFT is also an important factor in influencing the variation of plant functional traits (Verheijen et al., 2016; Loozen et al., 2020), thus the trait predictions were performed for each PFT individually. We used the 2015 land cover map at a 100 m spatial resolution to calculate the relative abundance of each PFT within 1 km grid cell, which was extracted from the Copernicus Global Land Service (CGLS-LC100, Version 3) (https://land.copernicus.eu/global/products/lc) (Buchhorn et al., 2020). We focused on natural terrestrial vegetation, so all artificial land cover types (e.g., croplands) were thus eliminated in our dataset. Seven categories were included: evergreen needleleaf forest (ENF), evergreen broadleaf forest (EBF), deciduous needleleaf forest (DNF), deciduous broadleaf forest (DBF), shrubland (SHL), grassland (GRL) and bare/sparse vegetation.

2.4 Model fitting and validation

To predict spatial patterns of plant functional traits, we used two machine learning models, i.e., random forest and boosted regression trees.

Random forest is an ensemble machine learning method based on classification and regression trees using collections of regression trees to classify observations according to a set of predictive variables (Breiman, 2001). This method repeatedly constructs a set of trees from random samples of training data, and the final prediction is produced by integrating the results of all individual trees, which makes it a robust method. The model is controlled by two main parameters: the number of sampled variables (mtry) and the number of trees (ntree). The mtry was set to range from 1 to 57 (at an interval of 1), and the ntree was set as 500, 1000, 2000, 5000 and 10000 in subsequent runs. This analysis was performed using the 'randomForest' function in the 'randomForest' package (Liaw and Wiener, 2002).

Boosted regression trees are machine learning methods based on generalized boosted regression models and using a boosting algorithm to combine many sample tree models to optimize predictive performance (Elith et al., 2006). There is no need for prior data transformation or the elimination of outliers, and this method can fit complex non-linear relationships while automatically handling interaction effects between predictors (Elith et al., 2008). The four parameters to optimize in these models are the number of trees, interaction depth, learning rate and bag fractions. We varied the parameter settings to find the optimal parameter combination that achieves minimum predictive error. The number of trees was set to 3000, the interaction depth varied from 1 to 7 (at an interval of 1), the learning rate was set to 0.001, 0.01, 0.05 and 0.1, and the bag fraction was set to 0.5, 0.6, 0.7 and 0.75. PFT was used as a dummy variable in the boosted regression trees models. This analysis was conducted using the 'gbm' function in the 'gbm' package (Ridgeway, 2006).

We built separate predictive model for each plant functional trait. To select the optimal parameter combination and to evaluate the final model performance for each trait, we calibrated the models 10 times using randomly selected 80% of the data for training models and validating against the remaining 20% based on cross-validation (Table B3 in Appendix B). The predictive performance was evaluated by regressing the predicted and observed trait values from all repetitions of the cross-validation. The fitting performance of the random forest and boosted regression trees was evaluated using determinate coefficient (R^2), normalized root-mean-square error (NRMSE) and mean absolute error (MAE). These scores are calculated following Eq. (1), Eq. (2) and Eq. (3):

$$R^2 = 1 - \frac{\sum_{i=1}^{n}(p_i - o_i)^2}{\sum_{i=1}^{n}(p_i - \hat{o_i})^2} \tag{1}$$

$$\mathrm{NRMSE} = \frac{\sqrt{\frac{1}{n}\sum_{i=1}^{n}(p_i - o_i)^2}}{p_{max} - p_{min}} \tag{2}$$

$$MAE = \frac{1}{n}\sum_{i=1}^{n}|o_i - p_i| \tag{3}$$

where p_i and o_i are the predictive values and observed values, respectively; $\hat{o_i}$ is the mean of the observed values.

To quantify the relative importance of each predictor across the two models consistently, we used the method proposed by Thuiller et al. (2009). This method applies correlation between the standard predictions fitted with the original data and predictions where the variable under investigation has been randomly permutated. If the correlation is high, which indicates little difference between the two predictions, the variable permutated is considered not important for the model. This step was repeated multiple times for each predictor, and the mean correlation coefficient over runs was recorded. Then the relative importance of each predictor was quantified as one minus the Spearman rank correlation coefficient (see Boonman et al., 2020). In addition, we used generalized additive models to fit the relationships between plant functional traits and the most important variables using the 'gam' function in the 'mgcv' package.

2.5 Generation of plant functional trait maps and model performance

The generation of spatial maps of plant functional traits was performed in three steps. First, we predicted trait values for each natural PFT (i.e., EBF, ENF, DBF, DNF, SHL and GRL) within 1 km grid cell separately. Second, the abundance of individual natural PFT within 1 km grid cell was estimated using a land cover map with a spatial resolution of 100 m. Third, refer to the Eq. (4) that has been widely applied in a community (Garnier et al., 2004), the final trait value in a given 1 km grid cell was calculated as the sum of the predicted trait values multiplying by corresponding abundance of each natural PFT.

$$\mathrm{CWM} = \sum_{i=1}^{n} W_i X_i \tag{4}$$

where *n* is the total number of PFT in a given grid; W_i is the relative abundance of the *i*th natural PFT; and X_i is the predicted trait value of the *i*th natural PFT.

To reduce the variability of different single-models and to construct a more stable and accurate model, the ensemble model was further applied to merge the predictions of random forest and boosted regression trees according to their cross-validated R^2 values. The predicted value of ensemble model was calculated in a given grid cell as described by Eq. (5) (Marmion et al., 2009). The model accuracy was calculated by regressing the predicted values of ensemble model against the observed trait values.

$$Pred\_EM_t = \frac{\sum_{m=1}^{2}(pred_{m,t} \times r_{m,t}^2)}{\sum_{m=1}^{2} r_{m,t}^2} \tag{5}$$

where $Pred\_EM_t$ is the predicted value of *t* trait in ensemble model; $pred_{m,t}$ is the predicted value of *t* trait in *m* model; $r_{m,t}^2$ is the cross-validated R^2 of *t* trait in *m* model.

To evaluate the model performance (i.e., the variability in the prediction across models), the coefficient of variation (CV) was calculated as the difference between the predictions of random forest and boosted regression trees methods and ensemble model. CV is calculated as following Eq. (6):

$$CV_t = \frac{\sqrt{\frac{\sum_{m=1}^{2}(pred_{m,t} - obs_t)^2 * r_{m,t}^2}{\sum_{m=1}^{2} r_{m,t}^2}}}{obs_t} \tag{6}$$

where $pred_{m,t}$ is the predicted value of *t* trait in *m* model; obs_t is the value of *t* trait in ensemble model; $r_{m,t}^2$ is the cross-validated R^2 of *t* trait in *m* model.

2.6 Uncertainty assessments

Multivariate environmental similarity surface analysis (MESS) was used to identify the range of the extrapolated predictor values across locations in the plant trait dataset (Elith et al., 2010). This method is often used to evaluate the extent of extrapolation and the applicability domain. If the value is negative, this indicates that at a given grid cell, at least one predictor variable is outside the extent of the referenced predictor layer. This analysis was conducted using the 'mess' function in the 'dismo' package.

All analyses were performed in R 4.0.2 (R Core Team, 2020).

3 Results

3.1 Performance of prediction models

Cross-validation showed that the performance of the predictive models differed greatly among the plant functional traits (Table 2, Tables C1 and C2 in Appendix C). WD had the best performance in all three models, with R^2 values of 0.64, 0.68 and 0.67 for random forest, boosted regression trees and ensemble model, respectively. SLA and LPC had R^2 values greater than 0.45, while LDMC performed the worst, with R^2 values below 0.30.

Table 2 Results of plant functional traits for cross-validated R^2, NRMSE and MAE for random forest, boosted regression trees and ensemble model.

	Random forest			Boosted regression trees			Ensemble model		
Traits	R^2	NRMSE	MAE	R^2	NRMSE	MAE	R^2	NRMSE	MAE
SLA	0.48	0.22	5.10	0.48	0.20	5.08	0.49	0.21	5.07
LDMC	0.23	0.21	0.07	0.28	0.18	0.07	0.24	0.20	0.07
LNC	0.33	0.19	4.92	0.34	0.18	4.85	0.34	0.19	4.85
LPC	0.51	0.24	0.53	0.51	0.22	0.53	0.51	0.27	0.53
LA	0.37	0.45	26.76	0.39	0.51	27.47	0.40	0.58	26.59
WD	0.64	0.20	0.10	0.68	0.13	0.10	0.67	0.17	0.10

SLA, specific leaf area (m^2 kg^{-1}); LDMC, leaf dry matter content (g g^{-1}); LNC, leaf N concentration (mg g^{-1}); LPC, leaf P concentration (mg g^{-1}); LA, leaf area (cm^2); WD, wood density (g cm^{-3}); R^2, determinate coefficient; NRMSE, normalized root-mean-square error; MAE, mean absolute error.

3.2 Spatial patterns of predicted plant functional traits

There were relatively consistent spatial patterns for SLA, LNC and LPC, with high values in the northeastern and northwestern China and the southeastern Qinghai-Tibet Plateau, and low values in the southwestern China (Figs. 3a, 3c and 3d, Figs. D1, D2, D3, D5 and D6 in Appendix D). SLA and LPC increased with latitude, while LNC did not vary significantly along latitudinal gradient. For SLA, LNC and LPC, the variability was low among random forest, boosted regression trees and ensemble model, with an overall CV less than 0.30 (Figs. 4a, 4c and 4d). LDMC values were relatively high in most regions of China, and the low values were mainly located in the eastern Yunnan Province and the Loess Plateau (Fig. 3b, Figs. D1, D2 and D4 in Appendix D). LA showed high values in the northeastern and southern regions (except for the Sichuan Basin), and the southeastern Qinghai-Tibet Plateau (Fig. 3e, Figs. D1, D2 and D7 in Appendix D). The strong latitudinal gradient was observed in LA, where the values decreased with latitude.

The CV values of LPC decreased with latitude, but other traits did not show latitudinal patterns (Fig. 4). The CV values of LA were relatively high, especially in the northwestern China and the Inner Mongolia-Loess Plateau region (Fig. 4e). WD had high values in the northeastern and southern regions (Fig. 2f, Figs. D1, D2 and D8 in Appendix D), while CV values for WD were low throughout China (Fig. 4f).

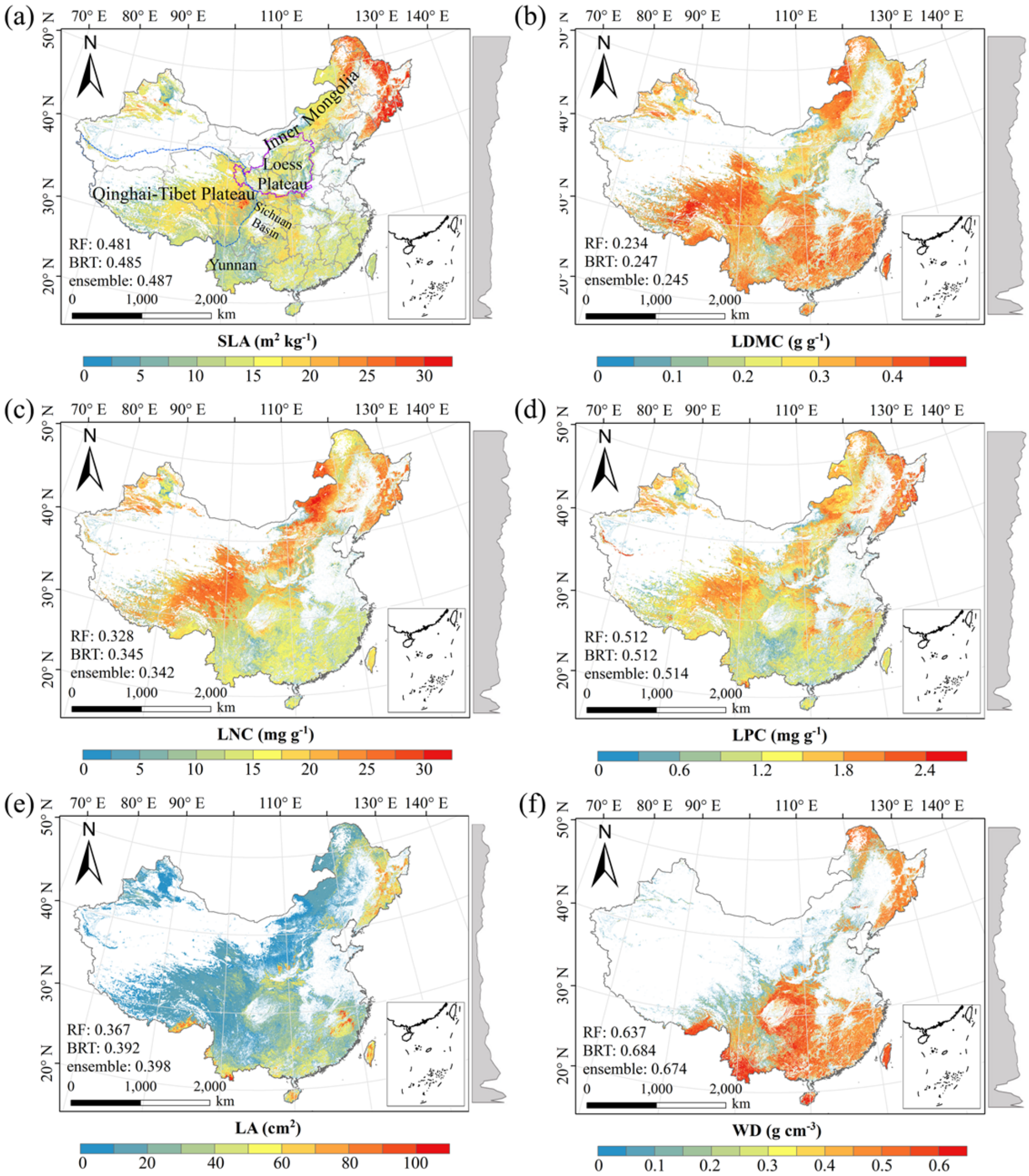

Figure 3. Spatial patterns of predicted plant functional traits in China based on the ensemble model. The grey curves to the right of the maps display trait distribution along with latitude. The white areas represent artificial land cover types and bare vegetation. The lines in grey, blue and purple represent the boundaries of province, the Qinghai-Tibet Plateau and the Loess Plateau, respectively. RF, random forest; BRT, boosted regression trees; ensemble, ensemble model; SLA, specific leaf area; LDMC, leaf dry matter content; LNC, leaf N concentration; LPC, leaf P concentration; LA, leaf area; WD, wood density.

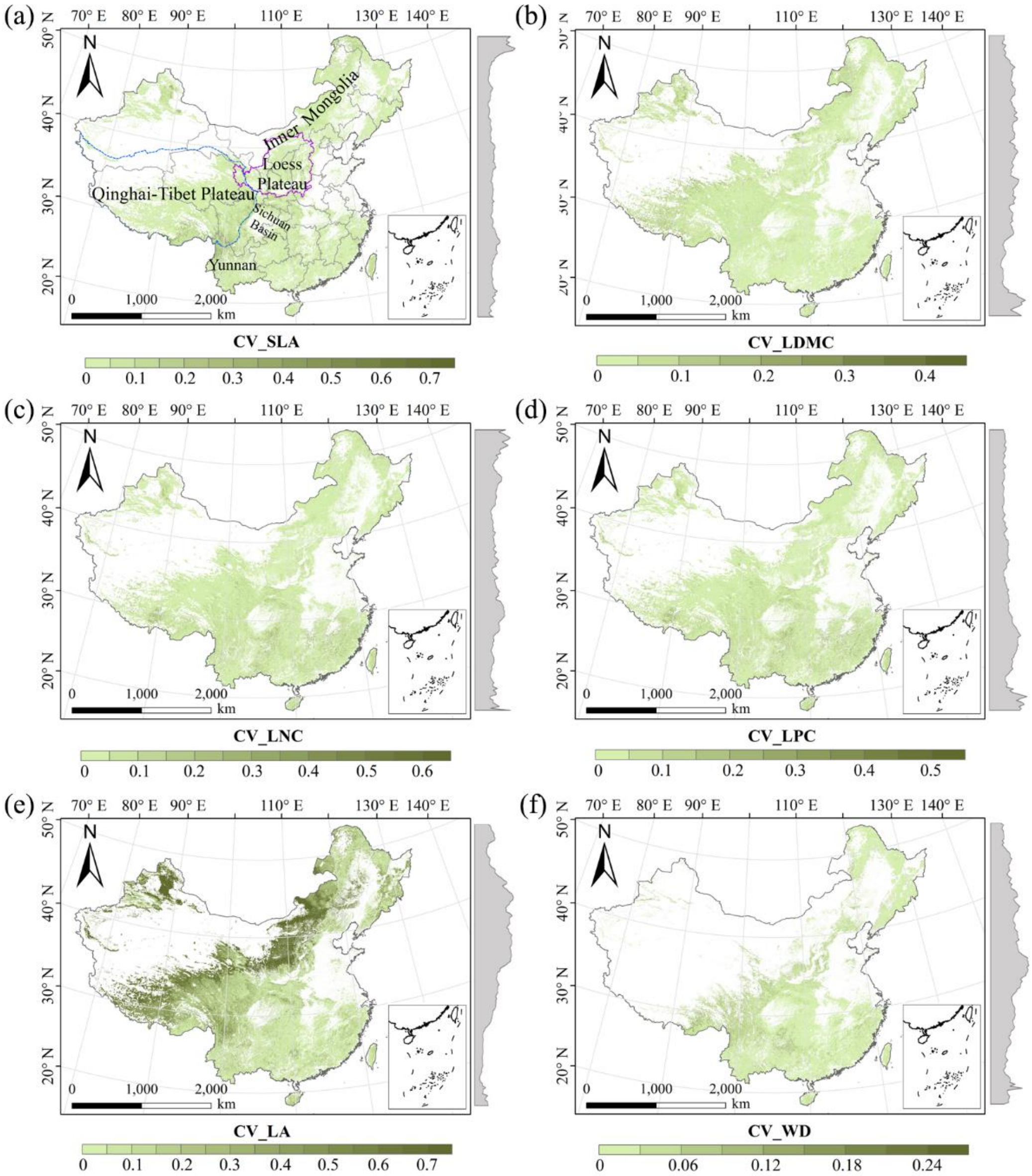

Figure 4. The variability in plant functional trait predictions among random forest, boosted regression trees and ensemble model. The grey curves to the right of the maps display coefficient of variation along with latitude. The white areas represent artificial land cover types and bare vegetation. The lines in grey, blue and purple represent the boundaries of province, the Qinghai-Tibet Plateau and the Loess Plateau, respectively. SLA, specific leaf area; LDMC, leaf dry matter content; LNC, leaf N concentration; LPC, leaf P concentration; LA, leaf area; WD, wood density.

3.3 Relative importance of predictive variables

The dominant factors explaining spatial variation differed greatly among plant functional traits (Table 3). Overall, climate variables were more important for predicting plant functional traits than were soil variables. Temperature variables (i.e., MAT, MDR and TS) showed close relationships with SLA, LDMC, LPC and WD, while precipitation variables (i.e., PS, PEQ, MAP and PDQ) were more important for predicting the spatial patterns of LNC, LPC and LA. RAD was the fourth most dominant factor in predicting the spatial patterns of SLA and WD. Elevation also played an important role in LDMC and LPC predictions. Within soil variables, soil nutrients (i.e., pH and SAP) showed close associations with SLA and LNC. In addition to the environmental variables, MTCI emerged as an important predictor for explaining SLA, LDMC and LA. Finally, EVI was the most important predictor for LA, and MIR in January and May were the primary predictors of WD. The relationships between plant functional traits and the most important variables were shown in Figs. E1 and E2 in Appendix E.

Table 3 List of the eight most important variables for plant functional trait predictions.

Rank	SLA	LDMC	LNC	LPC	LA	WD
1	SAP	MAT	PS	MDR	EVI5	MIR1
2	TS	Elevation	SAP	PDQ	PEQ	TS
3	blue9	MTCI5	pH	Elevation	MTCI9	MIR5
4	RAD	blue8	MDR	MIR8	NIR9	RAD
5	MTCI4	MTCI4	MAP	Tmax	AI	MIR6
6	MTCI6	MTCI6	PEQ	MTCI6	MTCI6	pH
7	Elevation	NIR1	MIR1	MIR7	MAP	red5
8	MTCI7	CEC	Tmax	MIR9	red5	PS

SLA, specific leaf area (m^2 kg^{-1}); LDMC, leaf dry matter content (g g^{-1}); LNC, leaf N concentration (mg g^{-1}); LPC, leaf P concentration (mg g^{-1}); LA, leaf area (cm^2); WD, wood density (g cm^{-3}); SAP, soil available P; TS, temperature seasonality; blue, blue reflectance; RAD, solar radiation; MTCI, MERIS terrestrial chlorophyll index; MAT, mean annual temperature; NIR, near-infrared reflectance; CEC, cation exchange capacity; PS, precipitation seasonality; MDR, mean diurnal range; MAP, mean annual precipitation; PEQ, precipitation of the wettest quarter of a year; MIR, middle infrared reflectance; Tmax, max temperature of the warmest month of a year; PDQ, precipitation of the driest quarter of a year; EVI, enhanced vegetation index; AI, aridity index; red, red reflectance.

3.4 Model performance

The distributions of the predicted values based on random forest, boosted regression trees and ensemble model were consistent with the original observations, especially the peak values (Fig. 5). The mean values of trait observations were relatively higher than those of the predicted values.

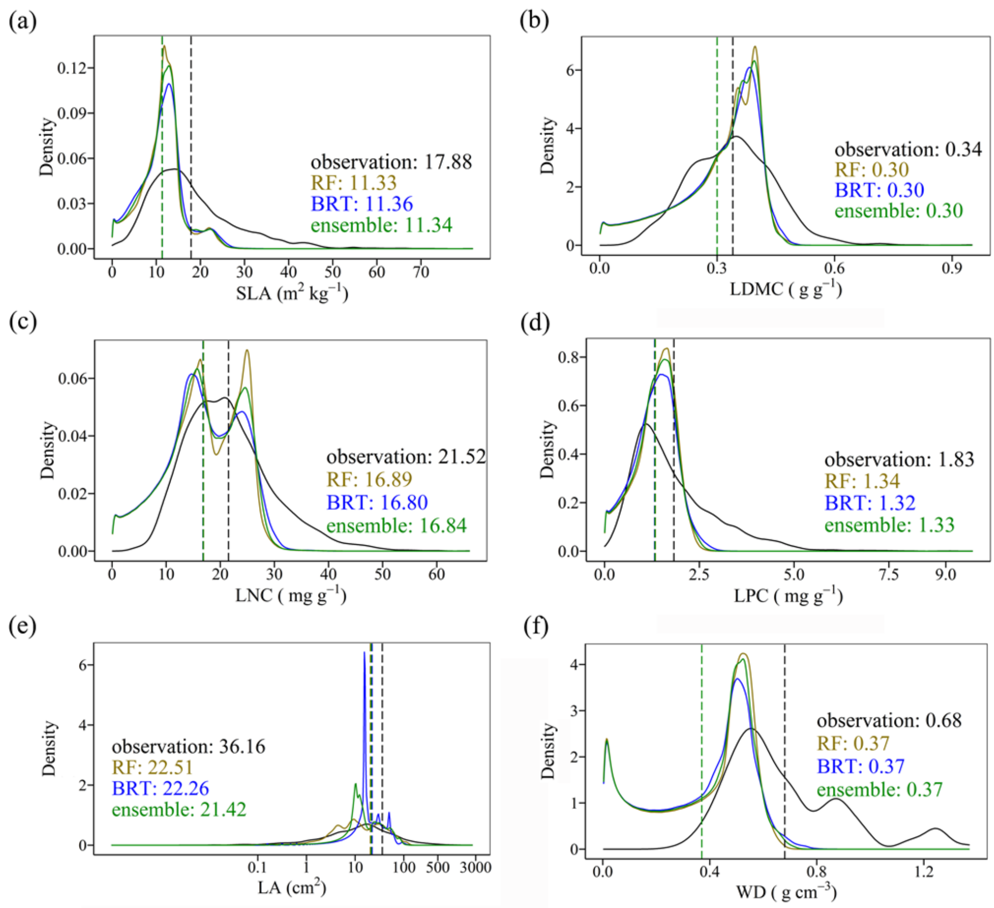

Figure 5. Comparison of trait distribution between observations and predictions in the three models. Each panel depicts the distribution of observations in solid black, of the random forest (RF) in yellow, of the boosted regression trees (BRT) in blue, and of the ensemble model in green. The dashed vertical lines indicate mean values. SLA, specific leaf area; LDMC, leaf dry matter content; LNC, leaf N concentration; LPC, leaf P concentration; LA, leaf area; WD, wood density.

3.5 Uncertainty assessments

The MESS values of all plant functional traits were positive in most regions, indicating a wide applicability domain of our models (Fig. 6). Nevertheless, trait predictions should be interpreted carefully for the northeastern China and the Qinghai-Tibet Plateau due to sparse samplings in these regions.

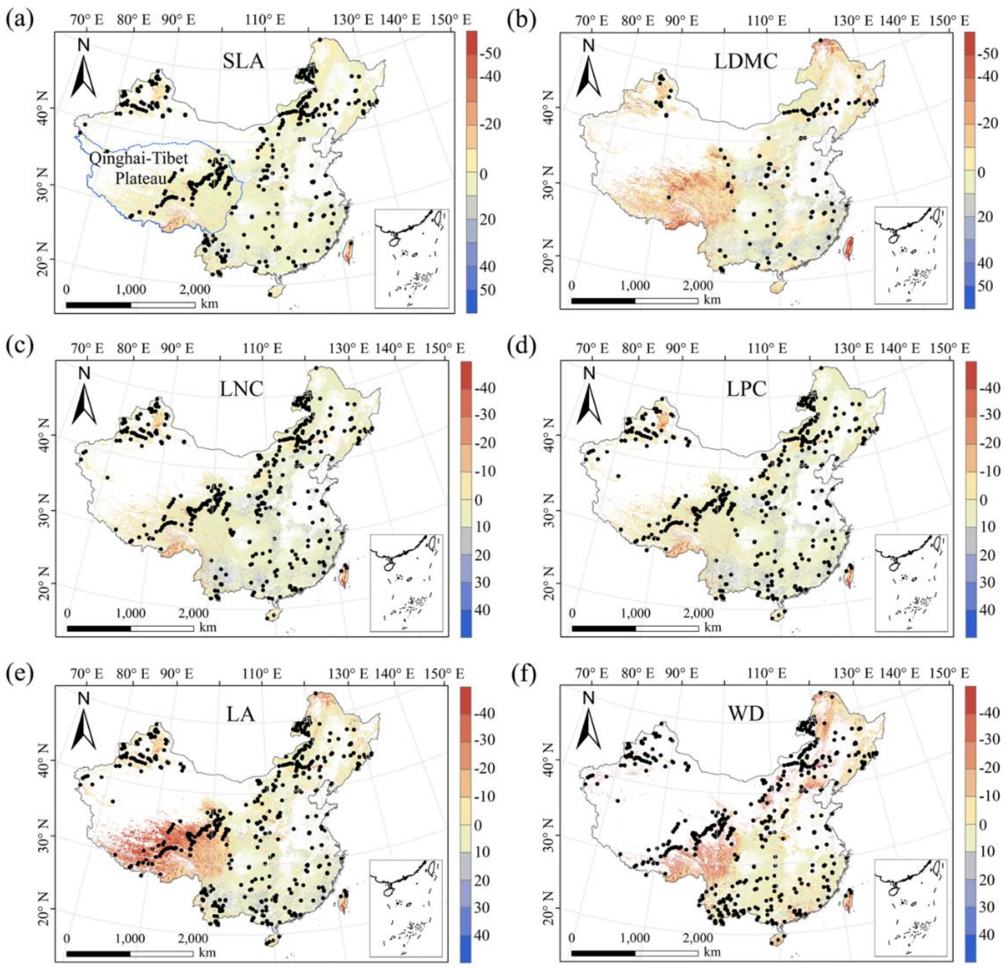

Figure 6. Multivariate environmental similarity surface (MESS) assessments for the six plant functional traits. The blue line represents the boundary of the Qinghai-Tibet Plateau. The black dots represent the locations of trait observations. More intense shades indicate greater similarity (blue) or difference (red) in environmental conditions of the location compared to the predictive factors covered by the training dataset. The white areas represent artificial land cover types and bare vegetation. SLA, specific leaf area; LDMC, leaf dry matter content; LNC, leaf N concentration; LPC, leaf P concentration; LA, leaf area; WD, wood density.

4 Discussion

4.1 Comparison with previous work

Our study predicted the spatial patterns of six key plant functional traits across China using machine learning methods and identified the applicability domain of the models. WD had the highest precision with an average of R^2 of 0.66, which was higher than the global WD prediction (Boonman et al., 2020). This improvement in precision may be attributed to the large number and dense occurrence of sample sites as well as the inclusion of vegetation indices in our study. In addition, SLA and LPC also showed good accuracy with R^2 values of 0.50, which was higher than that of Boonman et al. (2020) and consistent with that of Moreno-Martínez et al. (2018). However, LNC and LA showed relatively poor performance, which may be related to the reason that the two traits were more influenced by phylogeny than environmental variables (Yang et al., 2017; An et al., 2021). In addition, we found that mean values of trait predictions were lower than those of observations, which may be attributable to the reason that the mean values of trait observations were from the individual level, while the mean values of predicted values were based on the relative abundance of PFTs and corresponding predicted values within 1 km grid cell.

The frequency distributions of plant functional traits in China differed between our study and previous studies (Fig. 7, Fig. F1, Table F1 in Appendix F). Given that the spatial resolution of trait maps in most previous studies was 0.5° (except for Moreno-Martínez et al. (2018) and Vallicrosa et al. (2022)), we resampled the data products of previous studies and our study to 0.5° spatial resolution. The distributions in our study contained more predictions at lower values of SLA, LNC and LPC and were broader than those for SLA and LNC in previous global studies. However, the distribution of LNC in our study was consistent with that in the study of Vallicrosa et al. (2022) with a 1 km spatial resolution (Fig. F1 in Appendix F). LA in our study contained more predictions at higher values and was also broader than those in previous global studies. WD did not show lower and higher predicted values in this study, however, the WD values in the studies of Boonman et al. (2020) and Schiller et al. (2021) had more predictions at higher values and no lower values (< 0.30 g cm^{-3}). Our predicted values of SLA showed the highest spatial correlation with those of Dong et al. (2023), and LNC showed the strongest spatial correlation with those of Butler et al. (2017) (Table 4). LA and WD showed the best spatial correlation with those of Schiller et al. (2021), but LPC showed relatively weak spatial correlation with those of published studies.

In addition, we compared our results with the other studies focused on China. Yang et al. (2016) predicted the spatial distributions of leaf mass per area (i.e., 1/SLA) and LNC based on trait-environment relationships in China and had R^2 values of 0.13-0.16. The lower predictive precision may be because Yang et al. (2016) only used MAT, MAP and RAD as predictors in estimating the spatial patterns of leaf mass per area and LNC, which likely led to poor performance and low heterogeneity. These results also demonstrated the advantage of our methods in mapping the spatial patterns of plant functional traits at a regional scale.

Table 4 Spatial correlations for SLA, LNC, LPC, LA and WD between this study and previous trait maps, labelled by the first author of the corresponding publication (see Table F1 in Appendix F for citations)

Spatial correlation	Dong	Vallicrosa	Schiller	Boonman	Moreno	Madani	Butler	Bodegom
SLA	0.40		-0.08	0.33	0.24	0.14	-0.04	0.32
LNC	0.16	0.36	0.23	0.25			0.39	
LPC		0.14					0.06	
LA			0.51					
WD			0.65	0.11				

The spatial correlation of leaf dry matter content (LDMC) between our study and previous studies was not included, as the LDMC maps were not available. SLA, specific leaf area (m^2 kg^{-1}); LNC, leaf N concentration (mg g^{-1}); LPC, leaf P concentration (mg g^{-1}); LA, leaf area (cm^2); WD, wood density (g cm^{-3}).

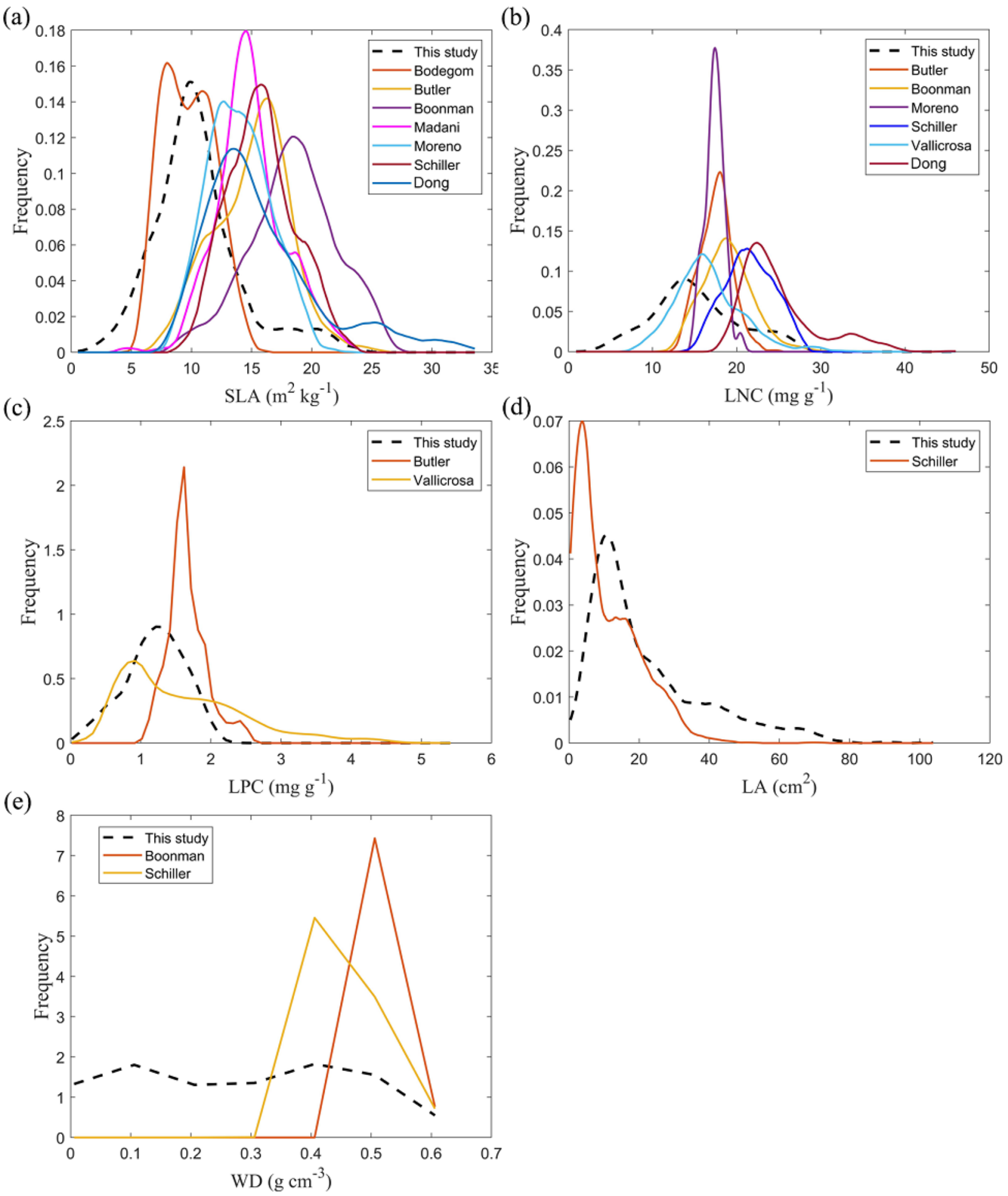

Figure 7. Frequency distributions of plant functional traits in our study ("This study", dashed black lines) and other trait maps identified by the first author of the corresponding publication (see Table F1 for citations). SLA, specific leaf area (m^2 kg^{-1}); LNC, leaf N concentration (mg g^{-1}); LPC, leaf P concentration (mg g^{-1}); LA, leaf area (cm^2); WD, wood density (g cm^{-3}).

4.2 Spatial patterns of plant functional traits in China

Our study revealed the spatial patterns of different plant functional traits across China, and the variability among the two machine learning methods was relatively low. We compared the spatial differences of trait maps between our study and previous studies at the global scale (Figs. F2-F6 in Appendix F). For example, our study showed high SLA values in the southeastern Qinghai-Tibet Plateau, which concurred with the global study of Boonman et al. (2020). The spatial difference of SLA between our study and van Bodegom et al. (2014) was relatively low, and the predicted values in most regions were slightly lower in our study than those in van Bodegom et al. (2014). The spatial pattern of difference in SLA between our study and Moreno et al. (2018), Bulter et al. (2017) and van Bodegom et al. (2014) was consistent, and the values were higher in the northeastern China and the southwestern Qinghai-Tibet Plateau in our study than those studies. Our study showed higher LNC values in the northern Inner Mongolia-the Loess Plateau-the eastern Qinghai-Tibet Plateau and the northwestern China than those global studies (Butler et al., 2017; Moreno-Martínez et al., 2018; Boonman et al., 2020; Vallicrosa et al., 2022; Dong et al., 2023), reflecting the consistent spatial pattern among these studies. However, Yang et al. (2016) predicted high LNC values in the northeastern and the northwestern China, the northern Inner Mongolia and the entire Qinghai-Tibet Plateau, and SLA and LNC had low heterogeneity overall. The discrepancy with Yang et al. (2016) may be attributed to spatial extrapolation based on trait-climate relationships with a low predictive precision. There was no consistent spatial pattern in LPC between our study and previous studies. Consistent with the global pattern (Wright et al., 2017), LA was larger in the southern regions than in the northern regions and showed a decreasing trend with latitude. In addition, LA and WD values in our study were lower in most regions than those ones at the global scale. These discrepancies between our study and previous studies at the global scale may be related to three reasons. First, there is bias in the available in-situ field measurement data from China in global studies, with a large gap in the western China for SLA and no data in China for WD (Boonman et al., 2020). Second, some trait-environment relationships may be scale-dependent (Bruelheide et al., 2018), and these studies we compared are from the global scale because the trait maps in China are not available. Third, the methods used for trait mapping were different among studies, including eco-evolutionary optimality models (Dong et al., 2023), Convolutional Neural Networks based on RGB photographs (Schiller et al., 2021), machine learning algorithms (Vallicrosa et al., 2022; Boonman et al., 2020) and multiple regression analysis (van Bodegom et al., 2014).

Moreover, our study also identified the applicability domain of our models for predicting the spatial patterns of plant functional traits across China. Five leaf traits and WD appeared to have poor applicability in the northeastern China and the Qinghai-Tibet Plateau, primarily due to sparse samplings. Future studies predicting plant functional traits across a large scale through remote sensing observations or other supplementary data will be needed to re-evaluate our results.

4.3 The role of predictive variables

Our study indicated that environmental variables were important for predicting the spatial patterns of plant functional traits, especially climate variables. Temperature variables were primary predictors for SLA, LDMC, LPC and WD. The relationships between leaf traits and temperature have been widely discussed in global and regional studies (Reich and Oleksyn, 2004; Bruelheide et al., 2018). The positive linkage between WD and temperature may be driven by changes in water viscosity. Plants can adapt to low water viscosity at high temperatures by reducing the diameter and density of their vessels and thickening cell walls (Roderick and Berry, 2002; Thomas et al., 2004). Precipitation variables were important predictors for leaf nutrient traits and LA. For example, precipitation of the wettest quarter of a year was the factor that most influenced LA variation, which has been confirmed by a previous study (An et al., 2021). A smaller LA could be an adaptive strategy to decrease water loss via reducing the surface area for transpiration under dry environmental conditions (Du et al., 2019). Although the effects of soil on trait predictions were relatively weak, we found that SAP and pH played key roles in SLA and LNC predictions. These results were similar with the previous studies reporting that soil pH was an important driver of trait variation at the global scale and in tundra regions (Maire et al., 2015; Kemppinen et al., 2021). Additionally, from the perspective of cost-efficient theory, the strong effects of SAP reflected that high SLA may be an adaptation for facilitating soil exploration more efficiently in fertile soils (Freschet et al., 2010).

Vegetation indices have recently been proposed as important predictors of spatial patterns of plant functional traits (Loozen et al., 2018). Our results corroborated these findings and further suggested that EVI, MTCI and MIR reflectance were important predictors in models. Here, the underlying mechanisms between vegetation indices and plant functional traits were not further discussed due to their complexity. However, our results indicated that vegetation indices and NIR reflectance were not key predictors of LNC estimation, which contrasted the findings from global and regional studies (Wang et al., 2016; Loozen et al., 2018; Moreno-Martínez et al., 2018). This may be related to the multitude of factors that influence the relationships between LNC and vegetation indices and NIR reflectance, such as forest type and canopy structure (Dahlin et al., 2013).

4.4 Uncertainties

Although our study mapped the spatial patterns of key functional traits in terrestrial ecosystems across China through large-scale field investigations and compared the predictions with previous studies at global and regional scales, there persisted some uncertainties in the interpretation of these results. First, the predictive ability of models was relatively worse for certain traits, especially LDMC. Beyond the environmental effects, the variation in plant functional traits is also regulated by phylogenetic structure among plant species (e.g., family, order and phylogenetic clade) (Li et al., 2017). Consequently, incorporating phylogenetic information will be a promising avenue for further improving the accuracy of spatial predictions of plant functional traits (Butler et al., 2017). A second potential issue is sampling bias; there are major spatial gaps in field investigations in the northeastern China and the Qinghai-Tibet Plateau. Due to the few measurements for shrubs and herbs, WD data is mainly confined to eastern forests, and the overall quantity of WD data is much lower than that of leaf traits, even in the TRY database. The environmental information of sampling sites was not always obtained from original literature, thus using the public environmental products is a common resolution in large-scale plant trait studies (Boonman et al., 2020; Vallicrosa et al., 2022). Such mismatch between in-situ trait measurements and predictors should be resolved in further work. Finally, an additional key challenge in data availability must be resolved to scale up from the species to the community levels, in particular with data surrounding species co-occurrence and their relative cover or abundance in ecological communities (He et al., 2023). For example, Global biodiversity data (e.g., sPlot and Global Biodiversity Information Agency databases) that contains information on species occurrence or the proportion of species in a community has the potential for enabling the calculation of community-weighted trait values and the re-evaluation of our results in future work (Telenius, 2011; Bruelheide et al., 2019). The lack of consistent time period and spatial resolution of predictors due to limitation of data availability is a key challenge in the spatial mapping of plant functional traits. In addition, although WorldClim version 2.1 product has high spatial resolution and includes various aspects of climatic parameters, there exists certain limitation and uncertainty in predicting trait maps. Therefore, integrating satellite remote sensing monitoring methods with in-situ trait data can also provide an effective way to estimate and assess the species diversity at large scales (Cavender-Bares et al., 2022).

4.5 Potential applications

Maps of these key functional traits in terrestrial ecosystems highlighted large-scale variability in space, which will significantly advance ecological analyses and future interdisciplinary research. First, using the spatially continuous trait maps, one can optimize and develop trait-flexible vegetation models to reduce uncertainty of conventional vegetation models based on PFTs, which allows for exploration of the community assembly rules based on how plants with different trait combinations perform under a given set of environmental conditions (Berzaghi et al., 2020). When trait-flexible vegetation models are available, incorporating trait maps into models will bridge the gap for vegetation classifications and predictions of vegetation distribution under global change (van Bodegom et al., 2012; Yang et al., 2019). Second, most studies focused on the effects of plant functional traits on ecosystem carbon processes at individual, species and community scales, while how such effects scale up to regional or larger scales remains challenging. In addition, the assessments of China's terrestrial ecosystem carbon sink have large uncertainties (Piao et al., 2022). The spatial continuous trait maps will provide an effective way to link ecosystem characteristics to ecosystem carbon sink estimates in China (Madani et al., 2018; Šímová et al., 2019). These analyses will help shed light on the mechanisms underlying plant functional traits and terrestrial ecosystem carbon storage at a large scale.

5 Data availability

The original plant functional trait data collected in this study that was used for machine learning models (named by Data file used for machine learning models.csv) and final maps of plant functional traits in a GeoTIFF format (named by plant functional trait category) are now available for the private link https://figshare.com/s/c527c12d310cb8156ed2 (An et al., 2023). Once the article is accepted, we will publicly publish the data at the figshare website.

6 Conclusions

We generated a set of spatial continuous trait maps at a 1-km spatial resolution using machine learning methods in combination with field measurements, environmental variables and vegetation indices. Models for leaf traits (except for LDMC) and WD showed good accuracy and robustness, whereas models of LDMC had relatively poor precision and robustness. Temperature variables were the most important predictors for leaf traits (except for LA) and WD, and precipitation variables were the most important predictors for leaf nutrient traits and LA. We caution that plant functional trait predictions should be interpreted carefully for the northeastern China and the Qinghai-Tibet Plateau. The spatial continuous trait maps generated in our study are complementary to current terrestrial in-situ observations and offer new avenues for predicting large-scale changes in vegetation and ecosystem functions under climate scenarios in China.

Appendix A Data collection from literature

An H. and Shangguan Z. P. Photosynthetic characteristics of dominant plant species at different succession stages of vegetation on Loess Plateau. Chinese Journal of Applied Ecology, 2007, 18, 1175-1180.

Bai K. D., Jiang D. B., Wan C. X. Photosynthesis-nitrogen relationship in evergreen and deciduous tree species at different altitudes on Mao'er Mountain, Guangxi. Acta Ecologica Sinica, 2013, 33, 4930-4938.

Bai W. J., Zheng F. L., Dong L. L., et al. Leaf traits of species in different habits in the water-wind erosion region of the Loess Plateau. Acta Ecologica Sinica, 2010, 30, 2529-2540.

Chai Y F., Shang H. L., Zhang X. F., et al. Ecological variations of woody species along an altitudinal gradient in the Qinling Mountains of Central China: area-based versus mass-based expression of leaf traits. Journal of Forestry Research, 2021, 32, 599-608.

Chang Y. N., Zhong Q. L., Cheng D. L., et al. Stoichiometric characteristics of C, N, P and their distribution pattern in plants of *Castanopsis carlesii* natural forest in Youxi. Journal of Plant Resources and Environment, 2013, 22, 1-10.

Chen F. Y., Luo T. X., Zhang L., et al. Comparison of leaf construction cost in dominant tree species of the evergreen broadleaved forest in Jiulian Mountain, Jiangxi Province. Acta Ecologica Sinica, 2006, 26, 2485-2493.

Chen H. Y., Huang Y. M., He K. J., et al. Temporal intraspecific trait variability drives responses of functional diversity to interannual aridity variation in grasslands. Ecology and Evolution, 2018, 9, 5731-5742.

Chen L. X., Xiang W. H., Wu H. L., et al. Tree growth traits and social status affect the wood density of pioneer species in secondary subtropical forest. Ecology and Evolution, 2017, 7, 5366-5377.

Chen L., Yang X. G., Song N. P., et al. Leaf water uptake strategy of plants in the arid-semiarid region of Ningxia. Journal of Zhejiang University, 2013, 39, 565-574.

Chen Y. H., Han W. X., Tang L. Y., et al. Leaf nitrogen and phosphorus concentrations of woody plants differ in responses to climate, soil and plant growth form. Ecography, 2011, 36, 178-184.

Cheng J. H, Chu P. F., Chen D. M., et al. Functional correlations between specific leaf area and specific root length along a regional environmental gradient in Inner Mongolia grasslands. Functional Ecology, 2016, 30, 985-997.

Cheng W., Yu C. H., Xiong K. N., et al. Leaf functional traits of dominant species in karst plateau-canyon areas. Guihaia, 2019, 39, 1039-1049.

Dong H. and Shekhar R. B. Negative relationship between interspecies spatial association and trait dissimilarity. Oikos, 2019, 128, 659-667.

Dong T. F., Feng Y. L., Lei Y. B., et al. Comparison on leaf functional traits of main dominant woody species in wet and dry habitats. Chinese Journal of Ecology, 2012, 31, 1043-1049.

Du H. D. Ecological responses of foliar anatomical structural & physiological characteristics of dominant plants at different site conditions in north Shaanxi Loss Plateau. 2010, Graduation Thesis.

Fan Z. X., Zhang S. B., Hao G. Y., et al. Hydraulic conductivity traits predict growth rates and adult stature of 40 Asian tropical tree species better than wood density. Journal of Ecology, 2012, 100, 732-741.

Feng J B., Fan S. X., Hou Y. F., et al. Interspecific and intraspecific variation of leaf function traits of herbaceous plants in a forest-steppe zone, Hebei Province, China. Journal of Northeast Forestry University, 2021, 49, 23-28.

Feng Q. H. The study on the response of foliar δ13C of different life from plants to altitude in subalpine area of Western Sichuan, China. 2011, Graduation Thesis.

Fu P. L., Zhu S. D., Zhang J. L., et al. The contrasting leaf functional traits between a karst forest and a nearby non-karst forest in south-west China. Functional Plant Biology, 2019, 46, 907-915.

Gao S. P., Li J. X., Xu M. C., et al. Leaf N and P stoichiometry of common species in successional stages of the evergreen broad-leaved forest in Tiantong National Forest Park, Zhejiang Province, China. Acta Ecologica Sinica, 2007, 27, 947-952.

Geekiyanage N., Goodale, U. M., Cao, K. F., et al. Leaf trait variations associated with habitat affinity of tropical karst tree species. Ecology and Evolution, 2017, 8, 286-295.

Geng Y., Ma W. H., Wang L., et al. Linking above- and belowground traits to soil and climate variables: an integrated database on China's grassland species. Ecology, 2017, 98, 1471.

Guo F. C. The photosynthetic characteristics of precious broad-leaved tree species in south subtropics and their relationship with leaf functional traits. 2015, Graduation Thesis.

Guo W. J. Exploring the relationship between arbuscular mycorrhizal fungi and plant based on phylogeny and plant traits. 2015, Graduation Thesis.

Hau C. H. Tree seed predation on degraded hillsides in Hong Kong. Forest Ecology & Management. 1997, 99, 215-221.

He J. S., Wang Z. H., Wang X. P., et al. A test of the generality of leaf trait relationships on the Tibetan Plateau. New Phytologist, 2006, 170, 835-848.

He P. C., Wright I. J., Zhu S. D., et al. Leaf mechanical strength and photosynthetic capacity vary independently across 57 subtropical forest species with contrasting light requirements. New Phytologist, 2019, 223, 607-618.

He Y. T. Studies on physioecological traits of 30 plant species in the Subalpine Meadow of the Qinling Mountains. 2007, Graduation Thesis.

Hou M. M. Adaptive evolution of some species from sedges (*Carex Cyperaceae*) based on phylogeny and leaf functional traits to habitat in the Poyang Lake Area. 2017, Graduation Thesis.

Hou Y., Liu M. X., Sun H. R., et al. Response of plant leaf traits to microhabitat change in a subalpine meadow on the eastern edge of Qinghai-Tibetan Plateau, China. Chinese Journal of Applied Ecology, 2017, 28, 71-79.

Hu Z. Z., Michaletz S. T., Johnson D. J., et al. Traits drive global wood decomposition rates more than climate. Global Change Biology, 2018, 24, 5259-5269.

Hua L., He P., Goldstein G., et al. Linking vein properties to leaf biomechanics across 58 woody species from a subtropical forest. Plant Biology, 2019, 22, 212-220.

Huang J. J. and Wang X. H. Leaf nutrient and structural characteristics of 32 evergreen broad -leaved species. Journal of East China Normal University (Natural Science), 2003, 1, 92-97.

Huang Y. L. The research about the turnover patterns and moisture adaptation mechanism of major species on the South-North-facing slope. 2012, Graduation Thesis.

Iida Y., Kohyama T. S., Swenson N. G., et al. Linking functional traits and demographic rates in a subtropical tree community: the importance of size dependency. Journal of Ecology, 2014, 102, 641-650.

Jia Q. Q. Functional traits of fine roots and their relationship with leaf traits of 50 major species in a subtropical forest in Gutianshan. 2011, Graduation Thesis.

Jiang Y., Chen X., Ma J., et al., Interspecific and intraspecific variation in functional traits of subtropical evergreen and deciduous broadleaved mixed forests in karst topography, Guilin, Southwest China. Tropical Conservation Science, 2016, 9.

Jin Y., Wang C. K., Zhou Z. H., et al. Co-ordinated performance of leaf hydraulics and economics in 10 Chinese temperate tree species. Functional Plant Biology, 2016, 43, 1082-1090.

Jing G. H. Responses of grassland community structure and functions to management practices on the semi-arid area of Loess Plateau. 2017, Graduation Thesis.

Kang M. Spatial distribution pattern and its causes of woody plant functional traits in Tiantong region, Zhejiang Province. 2012, Graduation Thesis.

Krober W., Li Y., Hardtle W., et al. Early subtropical forest growth is driven by community mean trait values and functional diversity rather than the abiotic environment. Ecology and Evolution, 2015, 5, 3541-3556.

Krober W., Bohnke M., Welk E., et al. Leaf trait-environment relationships in a subtropical broadleaved forest in south-east China. PloS One, 2012, 7, e35742.

Krober W., Zhang, S. R. Ehmig, M., et al. Linking xylem hydraulic conductivity and vulnerability to the leaf economics spectrum-a cross-species study. PloS One, 2014, e109211.

Li F. Comparison of functional traits in semi-humid evergreen broad-leaved in Western Hill of Kunming. 2011, Graduation Thesis.

Li K. and Xiang W. H. Comparison of specific leaf area, SPAD value and seed mass among subtropical tree species in hilly area of Central Hunan, China. Journal of Central South University of Forestry & Technology, 2011, 31, 213-218.

Li L., McCormack M. L., Ma C.G., et al. Leaf economics and hydraulic traits are decoupled in five species-rich tropical-subtropical forests. Ecology Letters, 2015, 18, 899-906.

Li Q. Leaf functional traits and their relationships with environmental factors in Beishan Mountain of Jinhua, Zhejiang Province. 2020, Graduation Thesis.

Li S. J., Su P. X., Zhang H. N., et al. Characteristics and relationships of foliar water and leaf functional traits of desert plants. Plant Physiology Journal, 2013, 49, 153-160.

Li W. H., Xu F. W., Zheng S. X., et al. Patterns and thresholds of grazing-induced changes in community structure and ecosystem functioning: species-level responses and the critical role of species traits. Journal of Applied Ecology, 2017, 54, 963-975.

Li W. Q, Xu Q., Li J., et al. Quantification of ecotone width of returned forest land from farmland based on specific leaf area. Journal of West China Forestry Science, 2017, 46, 117-121.

Li X. F., Pei K. Q., Kery M., et al. Decomposing functional trait associations in a Chinese subtropical forest. PloS One, 2017, 12, e0175727.

Li X. F., Schmid B., Wang F., et al. Net assimilation rate determines the growth rates of 14 species of subtropical forest trees. PloS One, 2016, 11, e0150644.

Li X. L., Li X. H., Jiang D. M., et al. Leaf morphological characters of 22 compositae herbaceous species in Horqin sandy land. Chinese Journal of Ecology, 2005, 24, 1397-1401.

Li Y. H., Luo T. X., Lu Q., et al. Comparisons of leaf traits among 17 major plant species in Shazhuyu Sand Control Experimental Station of Qinghai Province. Acta Ecologica Sinica, 2005, 25, 994-999.

Li Y. L., Meng Q. T., Zhao X. Y., et al. Relationships of fresh leaf traits and leaf litter decomposition in Kerqin Sandy Land. Acta Ecologica Sinica, 2008, 28, 2486-2494.

Li Y., Yao J., Yang S., et al. Trait differences research on leaf function of Liaodong oak forest main species in Dongling mountain. Guangdong Agricultural Sciences, 2012, 23, 159-162, 171.

Liang X. Y., Ye Q., Liu H., et al. Wood density predicts mortality threshold for diverse trees. New Phytologist, 2021, 229, 3053-3057.

Li, R., Zhu, S., Chen, H. Y. H., et al. Are functional traits a good predictor of global change impacts on tree species abundance dynamics in a subtropical forest? Ecology Letters, 2015, 18, 1181-1189.

Li Y. Y., Shi H., Shao M. A. Cavitation resistance of dominant trees and shrubs in Loess hilly region and their relationship with xylem structure. Journal of Beijing Forestry University, 2010, 32, 8-13.

Lin G. G., Guo, D. L., Li, L., et al. Contrasting effects of ectomycorrhizal and arbuscular mycorrhizal tropical tree species on soil nitrogen cycling: the potential mechanisms and corresponding adaptive strategies. Oikos, 2018, 127, 518-530.

Liu C. H. and Li Y. Y. Relationship between leaf traits and PV curve parameters in the typical deciduous woody plants occurring in Southern Huanglong Mountain. Journal of Northwest Forestry University, 2013, 28, 1-5.

Liu G. F., Freschet G. T., Pan X., et al. Coordinated variation in leaf and root traits across multiple spatial scales in Chinese semi-arid and arid ecosystems. New Phytologist, 2010, 188, 543-553.

Liu G. F., Wang L., Jiang L., et al. Specific leaf area predicts dryland litter decomposition via two mechanisms. Journal of Ecology, 2017, 106, 218-229.

Liu J. H., Zeng D. H. and Don K. L. Leaf traits and their interrelationships of main plant species in southeast Horqin sandy land. Chinese Journal of Ecology, 2006, 25, 921-925.

Liu J. X., Chen J., Jiang M. X., et al. Leaf traits and persistence of relict and endangered tree species in a rare plant community. Functional Plant Biology, 2012, 39, 512-518.

Liu L. H. The traits and adaptive strategies of main herbaceous plants and lianas on micro-topographical units in Huangcangyu reserves of Anhui Province. 2012, Graduation Thesis.

Liu M. C., Kong D. L., Lu X. R., et al. Higher photosynthesis, nutrient- and energy-use efficiencies contribute to invasiveness of exotic plants in a nutrient poor habitat in northeast China. Physiologia Plantarum, 2017, 160, 373-382.

Liu R. H., Bai J. L., Bao H., et al. Variation and correlation in functional traits of main woody plants in the *Cyclobalanopsis glauca* community in the karst hills of Guilin, southwest China. Chinese Journal of Plant Ecology, 2020, 44, 828-841.

Liu W. D., Su J. R., Li S. F., et al. Stoichiometry study of C, N and P in plant and soil at different successional stages of monsoon evergreen broad-leaved forest in Pu'er, Yunnan Province. Acta Ecologica Sinica, 2010, 30, 6581-6590.

Liu X. C., Jia H. B., Wang Q. Y. Genetic variation and correlation in wood properties of Betula platyphlla in natural Stands. Journal of Northeast Forestry University, 2018, 36, 8-10.

Liu Y. Y. Spatial distribution and habitat associations of trees in a typical mixed broad-leaved Korean pine (*Pinus koraiensis*) forest. 2014, Graduation Thesis.

Luo Y. H., Cadotte M. W., Burgess K. S., et al. Greater than the sum of the parts: how the species composition in different forest strata influence ecosystem function. Ecology Letters, 2019, 22, 1449-1461.

Lv J. Z., Miao Y. M., Zhang H. F., et al. Comparisons of leaf traits among different functional types of plant from Huoshan Mountain in the Shanxi Province. Plant Science Journal, 2010, 28, 460-465.

Ma J., Wu L. F., Wei X., et al. Habitat adaptation of two dominant tree species in a subtropical monsoon forest: leaf functional traits and hydraulic properties. Guihaia, 2015, 35, 261-268.

Mo J. M., Zhang D. Q., Huang Z. L., et al. Distribution pattern of nutrient elements in plants of Dinghushan Lower Subtropical Evergreen Broad-Leaved Forest. Journal of Tropical and Subtropical Botany, 2000, 8, 198-206.

Niu C. Y., Meinzer F. C. and Hao G. Y. Divergence in strategies for coping with winter embolism among co-occurring temperate tree species: the role of positive xylem pressure, wood type and tree stature. Functional Ecology, 2017, 31, 1550-1560.

Niu D. C., Li Q., Jiang S. G., et al. Seasonal variations of leaf C:N:P stoichiometry of six shrubs in desert of China's Alxa Plateau. Chinese Journal of Plant Ecology, 2013, 37, 317-325.

Niu K. C., He J. S. and Lechowicz M. J. Grazing-induced shifts in community functional composition and soil nutrient availability in Tibetan alpine meadows. Journal of Applied Ecology, 2016, 53, 1554-1564.

Niu K. C., Zhang S. and Lechowicz M. Harsh environmental regimes increase the functional significance of intraspecific variation in plant communities. Functional Ecology, 2020, 34, 1666-1677.

Niu S. L. Photosynthesis research on the predominant legume species in Hunshandak Sandland. 2004, Graduation Thesis.

Qi L. X. Response of leaf traits of *Pinus mongoliensis* and *Pinus massoniana* to elevation gradient in Daiyun Mountain. 2015, Graduation Thesis.

Ren Q. J., Li Q. J., Bu H. Y., et al. Comparison of physiological and leaf morphological traits for photosynthesis of the 51 plant species in the Maqu alpine swamp meadow. Chinese Journal of Plant Ecology, 2015, 39, 593-603.

Ren Y. T. The study of leaf functional traits of typical plants across the Alashan Desert. 2017, Graduation Thesis.

Ren Y., Wei C. G. and Guo X. Y. Comparison on leaf function traits of six kinds of plant in Ordos. Journal of Inner Mongolia Forestry Science & Technology, 2019, 45, 43-46, 55.

Rios R. S., Salgado-Luarte C. and Gianoli E. Species divergence and phylogenetic variation of ecophysiological traits in lianas and trees. PloS One, 2007, 9, e99871.

Shang K. K. Differentiation and maintenance of relict deciduous broad-leaved forest patterns along micro-topographic gradient in subtropical area, East China. 2011, Graduation Thesis.

Song Y T. Study on functional plant ecology in Songnen Grassland Northeast China. 2012, Graduation Thesis.

Song Y T., Zhou D. W., Li Q., et al. Leaf nitrogen and phosphorus stoichiometry in 80 herbaceous plant species of

Songnen grassland in Northeast China. Chinese Journal of Plant Ecology, 2012, 36, 222-230.

Tan X. Y. Research on leaf functional diversity of forest communities in rainy area of south-west China. 2014, Graduation Thesis.

Tang Q. Q. Variation in functional traits of plants in the Subtropical Evergreen and Deciduous Broad-leaved Mixed Forest. 2016, Graduation Thesis.

Tang Y. Inter-specific variations and relationship in leaf traits of major temperate species in northern China. 2011, Graduation Thesis.

Tao J. P., Zuo J., He Z., et al. Traits including leaf dry matter content and leaf pH dominate over forest soil pH as drivers of litter decomposition among 60 species. Functional Ecology, 2019, 33, 1798-1810.

Tian M., Yu G. R., He N. P., et al. Leaf morphological and anatomical traits from tropical to temperate coniferous forests: Mechanisms and influencing factors. Scientific Reports, 2016, 6, 19703.

Wang B. Analysis of leaf functional traits of 13 species trees in northwestern Fujian Province. 2019, Graduation Thesis.

Wang B. B. A study on ecological stoichiometry of six kinds of dominant shrubs in Huangcangyu Nature Reserve. 2015, Graduation Thesis.

Wang G. H. Leaf trait co-variation, response and effect in a chronosequence. Journal of Vegetation Science, 2007, 18, 563-570.

Wang G. H., Liu J. L. and Meng T. T. Leaf trait variation captures climate differences but differs with species irrespective of functional group. Journal of Plant Ecology, 2015, 8, 61-69.

Wang J. Y., Wang S. Q., Li R. L., et al. C:N:P stoichiometric characteristics of four forest types' dominant tree species in China. Chinese Journal of Plant Ecology, 2011, 35, 587-595.

Wang K. B. Vegetation ecological features and net primary productivity simulation in Yanggou watershed in the Loess hill-gully areas of China. 2011, Graduation Thesis.

Wang S. S. The traits and adaptive strategies of main herbaceous plants and lianas on micro-topographical units in Longjishan reserves of Anhui Province. 2016, Graduation Thesis.

Wei L. P. Variations in functional traits of main tree species along tree-crown in broadleaved Korean Pine Forest in Jiaohe, Jilin Province. 2014, Graduation Thesis.

Wei L. P., Hou J. H. and Jiang S. S. Changes of leaf functional traits of two main species along tree height in broad-leaved Korean pine forest. Guangdong Agricultural Sciences, 2014, 12, 55-58, 71.

Wei L. Y. and Shangguan Z. P. Relation between specific leaf areas and leaf nutrient contents of plants growing on slopelands with different farming-abandoned periods in the Loess Plateau. Acta Ecologica Sinica, 2008, 28, 2526-2535.

Wei L. Y., Zhou J. W., Xiao H. G., et al. Variations in leaf functional traits among plant species grouped by growth and leaf types in Zhenjiang, China. Journal of Forestry Research, 2011, 28, 241-248.

Wu D. H., Pietsch K. A., Staab M., et al. Wood species identity alters dominant factors driving fine wood decomposition along a subtropical plantation forests tree diversity gradient in subtropical plantation forests. Biotropica, 2021, 53, 643-657.

Wu T. G., Chen B. F., Xiao Y. H., et al. Leaf stoichiometry of trees in three forest types in Pearl River Delta, South China. Chinese Journal of Plant Ecology, 2009, 34, 58-63.

Xie Y. J. The characteristics of 20 dominant plant functional traits in evergreen broad-leaf forest in Daming Mountain Nature Reserve, Guangxi. 2013, Graduation Thesis.

Xu M. F., Ke X. H., Zhang Y., et al. Wood densities of six hardwood tree species in Eastern Guangdong and influencing factors. Journal of South China Agricultural University, 2016, 37, 100-106.

Xu M. S., Zhao Y. T., Yang X. D., et al. Geostatistical analysis of spatial variations in leaf traits of woody plants in

Tiantong, Zhejiang Province. Chinese Journal of Plant Ecology, 2016, 40, 48-59.

Xu Y. Z. Biomass estimate and storage mechanisms in northern subtropical forest ecosystems, central China. 2016, Graduation Thesis.

Xun Y. H., Di X. Y. and Jin G. Z. Vertical variation and economic strategy of leaf trait of major tree species in a typical mixed broadleaved-Korean pine forest. Chinese Journal of Plant Ecology, 2020, 44, 730-741.

Yan E. R., Wang X. H., Guo M., et al. C:N:P stoichiometry across evergreen broad-leaved forests, evergreen coniferous forests and deciduous broad-leaved forests in the Tiantong region, Zhejiang Province, eastern China. Chinese Journal of Plant Ecology, 2010, 34, 48-57.

Yang S. The adaptive strategies of main herbaceous plants traits to different micro-topographical units in Dashushan Mountain, Hefei. 2017, Graduation Thesis.

Yang Y., Xu X., Xu M., et al. Adaptation strategies of three dominant plants in the trough-valley karst region of northern Guizhou Province, Southwestern China, evidence from associated plant functional traits and ecostoichiometry. Earth and Environment, 2020, 48, 413-423.

Yang Z., Fan S. X., Zhou B. C., et al. Leaf function and soil nutrient differences of dominant tree species on different slope aspects at the south foothills of Taihang Mountains. Journal of Henan Agricultural University, 2020, 54, 408-414.

Yin Q. L., Wang L., Lei, M. L., et al. The relationships between leaf economics and hydraulic traits of woody plants depend on water availability. Science of the Total Environment, 2018, 621, 245-252.

Yu Y. H., Zhong X. P. and Chen W. Analysis of relationship among leaf functional traits and economics spectrum of dominant species in northwestern Guizhou Province. Journal of Forest and Environment, 2018, 38, 196-201.

Yuan S. Preliminary research on plant functional traits and the capability of carbon sequestration of major tree species in Changbai Mountain Area. 2011, Graduation Thesis.

Zhang H., Chen H. Y. H., Lian J. Y., et al. Using functional trait diversity patterns to disentangle the scale-dependent ecological processes in a subtropical forest. Functional Ecology, 2018, 32, 1379-1389.

Zhang J. G., Fu S. L., Wen Z. D., et al. Relationship of key leaf traits of 16 woody plant species in Low Subtropical China. Journal of Tropical and Subtropical Botany, 2009, 17, 395-400.

Zhang J. L., Poorter L., Cao K. F. Productive leaf functional traits of Chinese savanna species. Plant Ecology, 2012, 213, 1449-1460.

Zhang J. Y. Comparative study on the different plant functional groups leaf traits at the Maoershan Region. 2008, Graduation Thesis.

Zhang Q. W., Zhu S. D., Jansen S., et al. Topography strongly affects drought stress and xylem embolism resistance in woody plants from a karst forest in Southwest China. Functional Ecology, 2020, 35, 566-577.

Zhang S. B. and Cao K. F. Stem hydraulics mediates leaf water status, carbon gain, nutrient use efficiencies and plant growth rates across dipterocarp species. Functional Ecology, 2009, 23, 658-667.

Zhang S. B., Cao K. F., Fan Z. X., et al. Potential hydraulic efficiency in angiosperm trees increases with growth-site temperature but has no trade-off with mechanical strength. Global Ecology and Biogeography, 2013, 22, 971-981.

Zhang Y., Ren Y. X., Yao J., et al. Leaf nitrogen and phosphorous stoichiometry of trees in *Pinus tabulaeformis* Carr stands, North China. Journal of Anhui Agricultural University, 2012, 39, 247-251.

Zhao Y. T., Ali, A. and Yan, E. R. The plant economics spectrum is structured by leaf habits and growth forms across subtropical species. Tree Physiology, 2016, 37, 173-185.

Zheng X. J., Li S. and Li Y. Leaf water uptake strategy of desert plants in the Junggar Basin, China. Chinese Journal of Plant Ecology, 2011, 35, 893-905.

Zheng Y. M. Carbon, nitrogen and phosphorus stoichiometry of plant and soil in the sandy hills of Poyang Lake. 2014, Graduation Thesis.

Zheng Z. X. Comparison of plant leaf, height and seed functional traits in dry-hot valleys. 2010, Graduation Thesis.

Zhou J. Y., He J. J., Guo Z. Y., et al. A study on specific leaf area and leaf dry matter content of five dominant species in Xiangshan Mountain, Huaibei City, Anhui Province. Journal of Huaibei Normal University (Natural Sciences), 2013, 34, 51-54.

Zhou X., Zuo X. A., Zhao X. Y., et al. Plant functional traits and interrelationship of 34 plant species in south central Horqin Sandy Land, China. Journal of Desert Research, 2015, 35, 1489-1495.

Zhu B. R., Xu B. and Zhang D. Y. Extent and sources of variation in plant functional traits in grassland. Journal of Beijing Normal University (Natural Science), 2011, 47, 485-489.

Zhu S. D., Song J. J., Li R. H., et al. Plant hydraulics and photosynthesis of 34 woody species from different successional stages of subtropical forests. Plant Cell and Environment, 2013, 36, 879-891.

Zhu X. B., Liu Y. M. and Sun S. C. Leaf expansion of the dominant woody species of three deciduous oak forests in Nanjing, East China. Chinese Journal of Plant Ecology, 2005, 29, 125-136.

Appendix B

Table B1 Summary of statistics in plant functional traits, environmental variables and geographical distribution in China.

Trait	Unit	Range	Mean	CV (%)	No. of species	Entries	Sites
SLA	$m^2\ kg^{-1}$	0.06–81.68	17.88	54.96	2463	9195	1032
LDMC	$g\ g^{-1}$	0.06–0.95	0.34	100.00	1582	3957	193
LNC	$mg\ g^{-1}$	3.41–66.02	21.52	37.44	2335	7407	567
LPC	$mg\ g^{-1}$	0.09–9.70	1.83	62.19	2074	6266	515
LA	cm^2	0.0033–2553.33	36.16	259.64	1838	5976	691
WD	$g\ cm^{-3}$	0.25–1.37	0.68	33.16	768	1788	639
Altitude	m	-144–5454					1430
MAT	°C	-12.07–24.32					1430
MAP	mm	15–2982					1430
Soil total N	$g\ kg^{-1}$	0.11–10.25					1430
Bulk density	$g\ cm^{-3}$	0.83–1.45					1430

SLA, specific leaf area; LDMC, leaf dry matter content; LNC, leaf N concentration; LPC, leaf P concentration; LA, leaf area; WD, wood density; MAT, mean annual temperature; MAP, mean annual precipitation.

Table B2 List of all predictors including environment and remote sensing variables used in this study.

Type of variables	Variable name	Abbreviations	Units	Time periods	Spatial resolution	Source
Climate	Mean annual temperature	MAT	°C	1970-2000	1 km	WorldClim version 2.1
	Mean diurnal range	MDR	°C	1970-2000	1 km	WorldClim version 2.1
	Temperature seasonality	TS	°C	1970-2000	1 km	WorldClim version 2.1
	Max temperature of the warmest month	Tmin	°C	1970-2000	1 km	WorldClim version 2.1
	Min temperature of the coldest month	Tmax	°C	1970-2000	1 km	WorldClim version 2.1
	Temperature annual range	TAR	°C	1970-2000	1 km	WorldClim version 2.1
	Isothermality	IS	%	1970-2000	1 km	WorldClim version 2.1
	Mean temperature of the wettest quarter	MTEQ	°C	1970-2000	1 km	WorldClim version 2.1
	Mean temperature of the driest quarter	MTDQ	°C	1970-2000	1 km	WorldClim version 2.1
	Mean temperature of the warmest quarter	MTWQ	°C	1970-2000	1 km	WorldClim version 2.1
	Mean temperature of the coldest quarter	MTCQ	°C	1970-2000	1 km	WorldClim version 2.1
	Mean annual precipitation	MAP	mm	1970-2000	1 km	WorldClim version 2.1
	Precipitation of the wettest month	PEM	mm	1970-2000	1 km	WorldClim version 2.1
	Precipitation of the driest month	PDM	mm	1970-2000	1 km	WorldClim version 2.1
	Precipitation seasonality	PS	%	1970-2000	1 km	WorldClim version 2.1
	Precipitation of the wettest quarter	PEQ	mm	1970-2000	1 km	WorldClim version 2.1
	Precipitation of the driest quarter	PDQ	mm	1970-2000	1 km	WorldClim version 2.1
	Precipitation of the warmest quarter	PWQ	mm	1970-2000	1 km	WorldClim version 2.1
	Precipitation of the coldest quarter	PCQ	mm	1970-2000	1 km	WorldClim version 2.1
	Aridity index	AI	/	1970-2000	1 km	Global CGIAR-CSI
	Solar radiation	RAD	$kJ\ m^{-2}\ day^{-1}$	1970-2000	1 km	WorldClim version 2.1
Topography	Elevation	/	m		1 km	SRTM 90m V4.1
Soil	Soil sand content	SAND	%	/	1 km	Shangguan et al. (2013)
	Soil silt content	SILT	%	/	1 km	Shangguan et al. (2013)
	Soil clay content	CLAY	%	/	1 km	Shangguan et al. (2013)
	Bulk density	BD	$g\ cm^{-3}$	/	1 km	Shangguan et al. (2013)
	Soil pH	pH	/	/	1 km	Shangguan et al. (2013)
	Soil organic matter	SOC	$g\ kg^{-1}$	/	1 km	Shangguan et al. (2013)
	Soil total N	STN	$g\ kg^{-1}$	/	1 km	Shangguan et al. (2013)
	Soil total P	STP	$g\ kg^{-1}$	/	1 km	Shangguan et al. (2013)
	Soil alkali-hydrolysable N	SAN	$mg\ kg^{-1}$	/	1 km	Shangguan et al. (2013)
	Soil available P	SAP	$mg\ kg^{-1}$	/	1 km	Shangguan et al. (2013)
	Soil available K	SAK	$mg\ kg^{-1}$	/	1 km	Shangguan et al. (2013)
	Cation exchange capacity	CEC	$me\ kg^{-1}$	/	1 km	Shangguan et al. (2013)

Continued

Type of variables	Variable name	Abbreviations	Units	Time periods	Spatial resolution	Source
EVI	MODIS EVI long-term monthly averages		/	2001-2018	1 km	MOD13A3 V006
NIR	MODIS NIR long-term monthly averages		/	2001-2018	1 km	MOD13A3 V006
MIR	MODIS MIR long-term monthly averages		/	2001-2018	1 km	MOD13A3 V006
Red	MODIS red long-term monthly averages		/	2001-2018	1 km	MOD13A3 V006
Blue	MODIS blue long-term monthly averages		/	2001-2018	1 km	MOD13A3 V006
MTCI	MTCI long-term monthly averages		/	2003-2011	4.63 km	MTCI level 3 product
Land cover	Land cover map		/	2015	100 m	Copernicus Global Land Service Collection 3

The vegetation indices are calculated as long-term monthly averages from 2001 to 2018, thus 12 variables of each vegetation index category are obtained.

Table B3 The number of samples of six plant functional traits used for model training (80%) and validation (20%).

Traits	No. of samples	No. of samples used for model training	No. of samples used for model validation
SLA	9195	7356	1839
LDMC	3957	3166	791
LNC	7407	5926	1481
LPC	6266	5013	1253
LA	5976	4781	1195
WD	1787	1430	357

SLA, specific leaf area (m^2 kg^{-1}); LDMC, leaf dry matter content (g g^{-1}); LNC, leaf N concentration (mg g^{-1}); LPC, leaf P concentration (mg g^{-1}); LA, leaf area (cm^2); WD, wood density (g cm^{-3}).

898

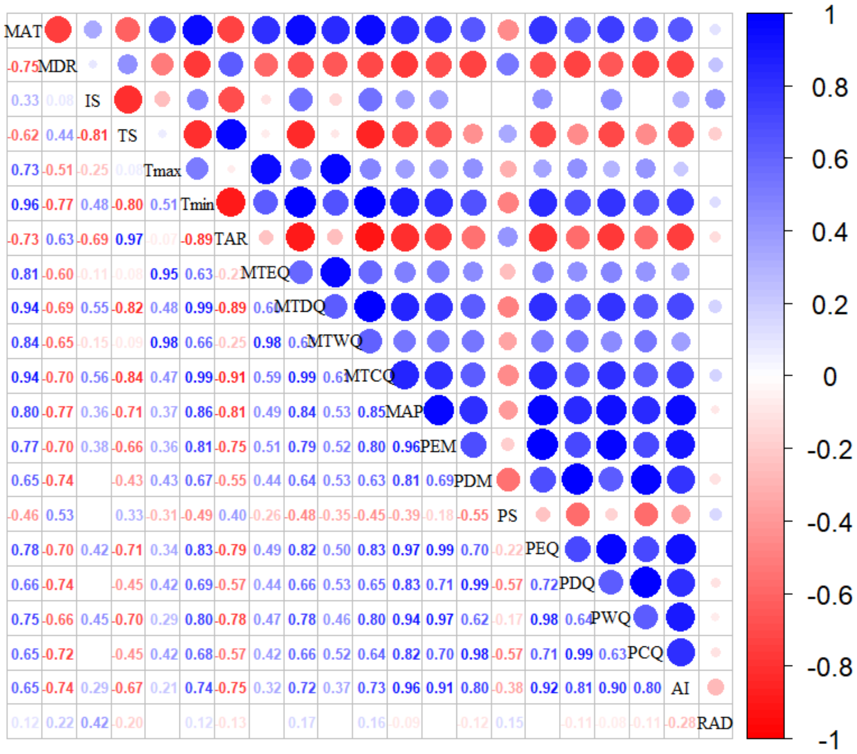

899 **Figure B1.** Correlations among climate variables. The blank indicates that the correlations are not
900 significant (P > 0.05). The size of the circles is proportional to the correlation coefficient. The
901 abbreviations of climate variables are seen in Table B2.

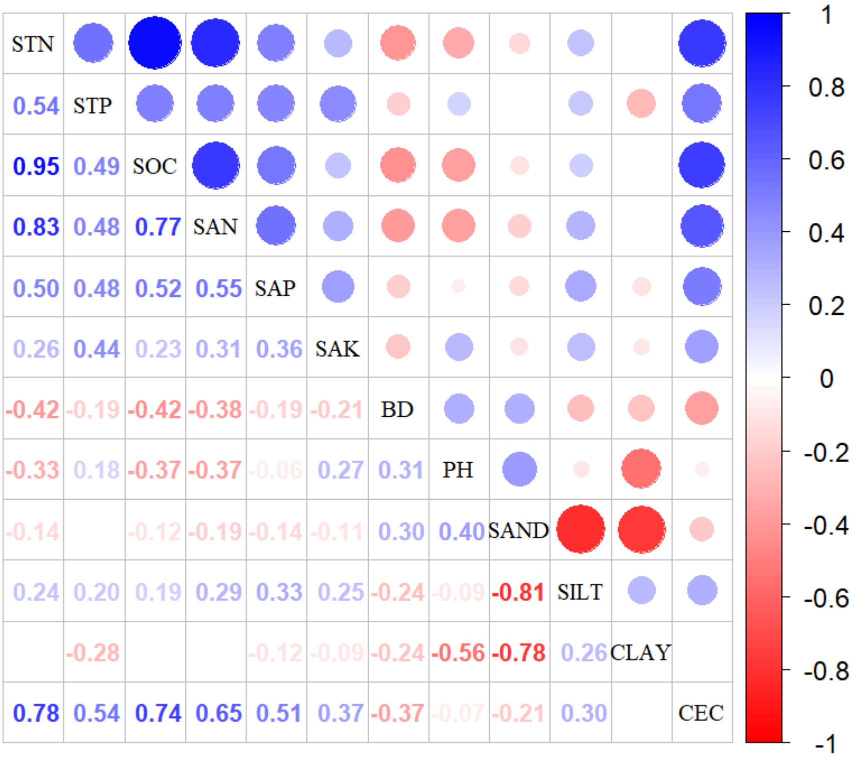

Figure B2. Correlations among soil variables. The blank indicates that the correlations are not significant ($P > 0.05$). The size of the circles is proportional to the correlation coefficient. The abbreviations of soil variables are seen in Table B2.

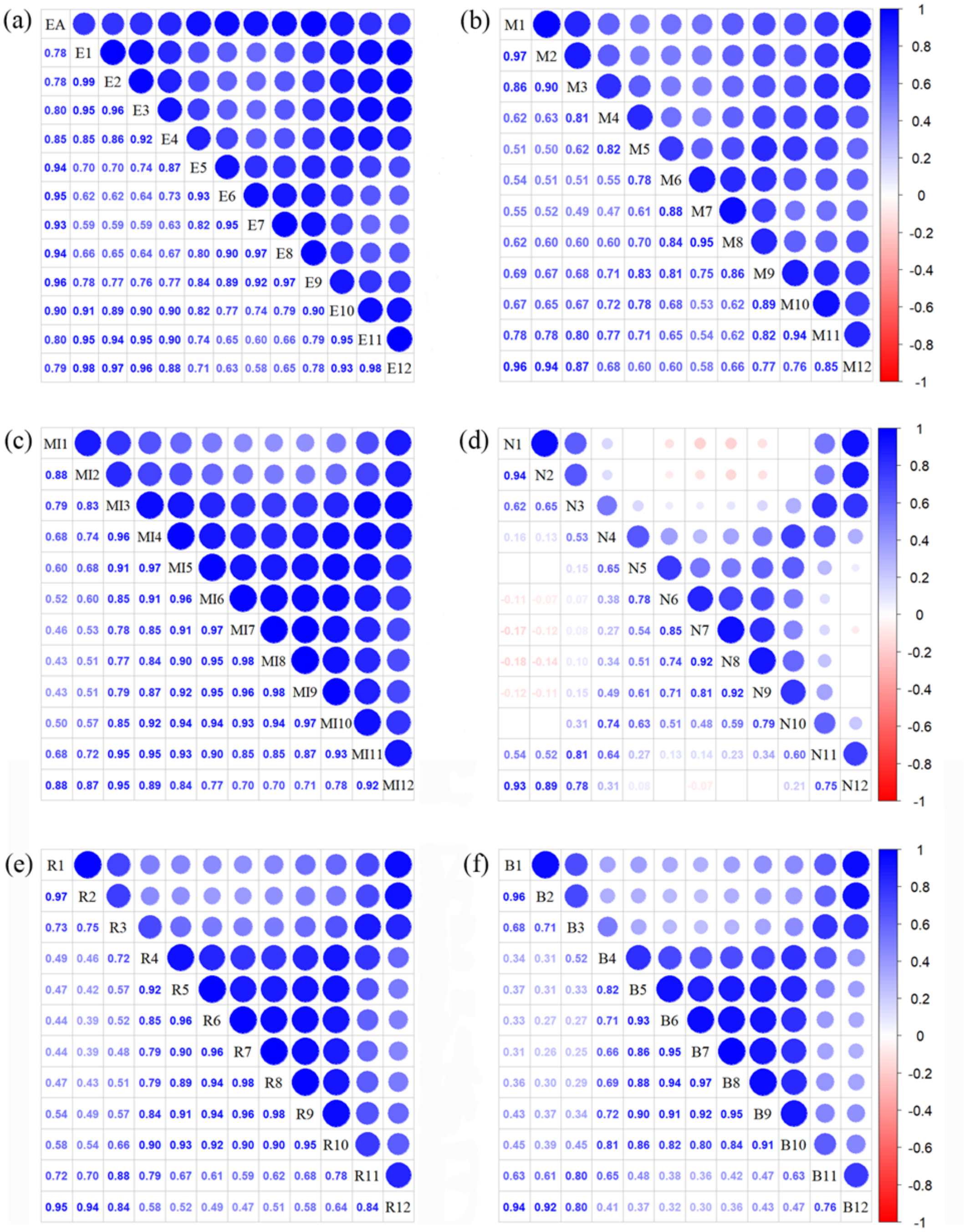

Figure B3. Correlations among monthly vegetation index variables. The blank indicates that the correlations are not significant ($P > 0.05$). The size of the circles is proportional to the correlation coefficient. (a) enhanced vegetation index (EVI); (b) MERIS terrestrial chlorophyll index (MTCI); (c) MIR reflectance; (d) NIR reflectance; (e) red reflectance; (f) blue reflectance.

Appendix C

Table C1 Optimal parameter combination and model performance of random forest for plant functional traits.

Traits	ntree	mtry	R^2	NRMSE	MAE
SLA	1000	24	0.48	0.22	5.13
LDMC	1000	11	0.23	0.20	0.07
LNC	1000	57	0.39	0.00	0.10
LPC	1000	20	0.59	0.05	0.13
LA	1000	18	0.28	0.48	26.62
WD	1000	9	0.53	0.02	0.07

SLA, specific leaf area; LDMC, leaf dry matter content; LNC, leaf N concentration; LPC, leaf P concentration; LA, leaf area; WD, wood density; R^2, determinate coefficient; NRMSE, normalized root-mean-square error; MAE, mean absolute error.

Table C2 Optimal parameter combination and model performance of boosted regression trees for plant functional traits.

Traits	n.tree	interaction depth	shrinkage	learning rate	bag fractions	R^2	NRMSE	MAE
SLA	3000	6	0.01	10	0.75	0.49	0.20	5.08
LDMC	3000	2	0.01	10	0.75	0.28	0.19	0.07
LNC	3000	6	0.01	10	0.70	0.41	0.00	0.10
LPC	3000	7	0.01	10	0.75	0.59	0.05	0.13
LA	3000	3	0.001	10	0.75	0.28	0.55	27.56
WD	3000	4	0.01	10	0.70	0.63	0.01	0.07

SLA, specific leaf area; LDMC, leaf dry matter content; LNC, leaf N concentration; LPC, leaf P concentration; LA, leaf area; WD, wood density; R^2, determinate coefficient; NRMSE, normalized root-mean-square error; MAE, mean absolute error.

Appendix D

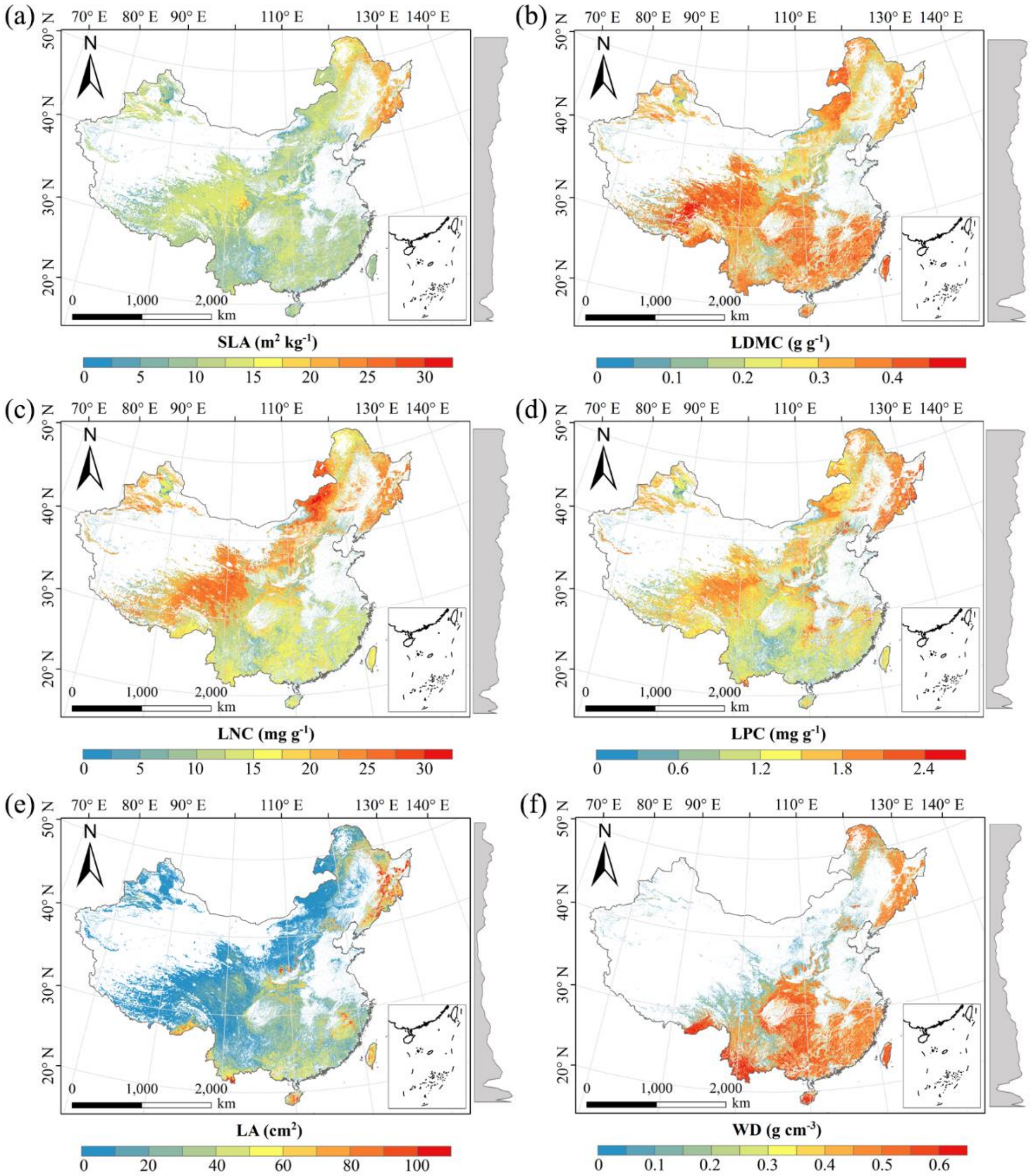

Figure D1. Spatial distributions of plant functional traits based on random forest. The grey curves on the right of maps are trait distribution along with latitude. The white areas represent artificial land cover types and bare vegetation. SLA, specific leaf area; LDMC, leaf dry matter content; LNC, leaf N concentration; LPC, leaf P concentration; LA, leaf area; WD, wood density.

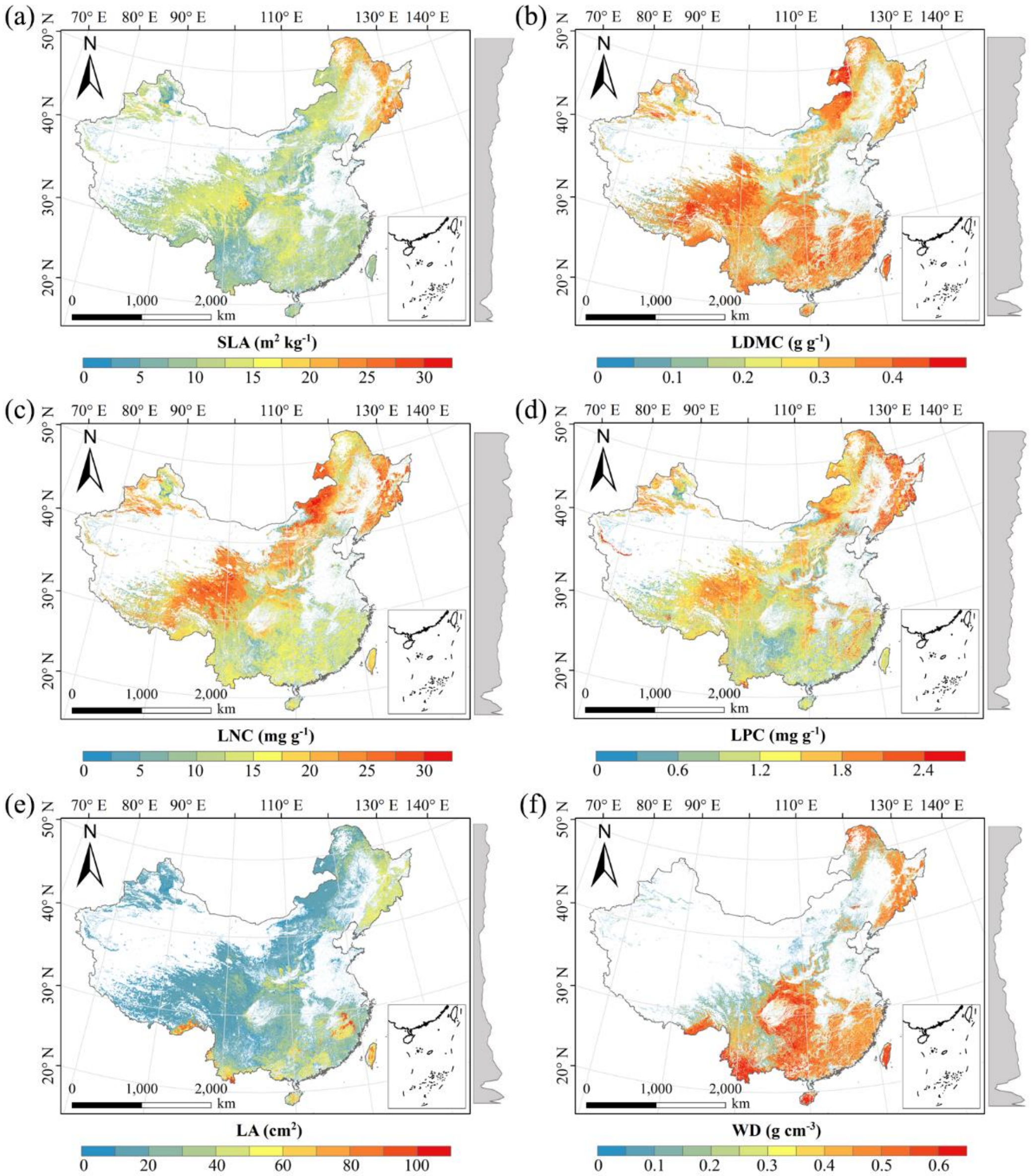

Figure D2. Spatial distributions of plant functional traits based on boosted regression trees. The grey curves on the right of maps are trait distribution along with latitude. The white areas represent artificial land cover types and bare vegetation. SLA, specific leaf area; LDMC, leaf dry matter content; LNC, leaf N concentration; LPC, leaf P concentration; LA, leaf area; WD, wood density.

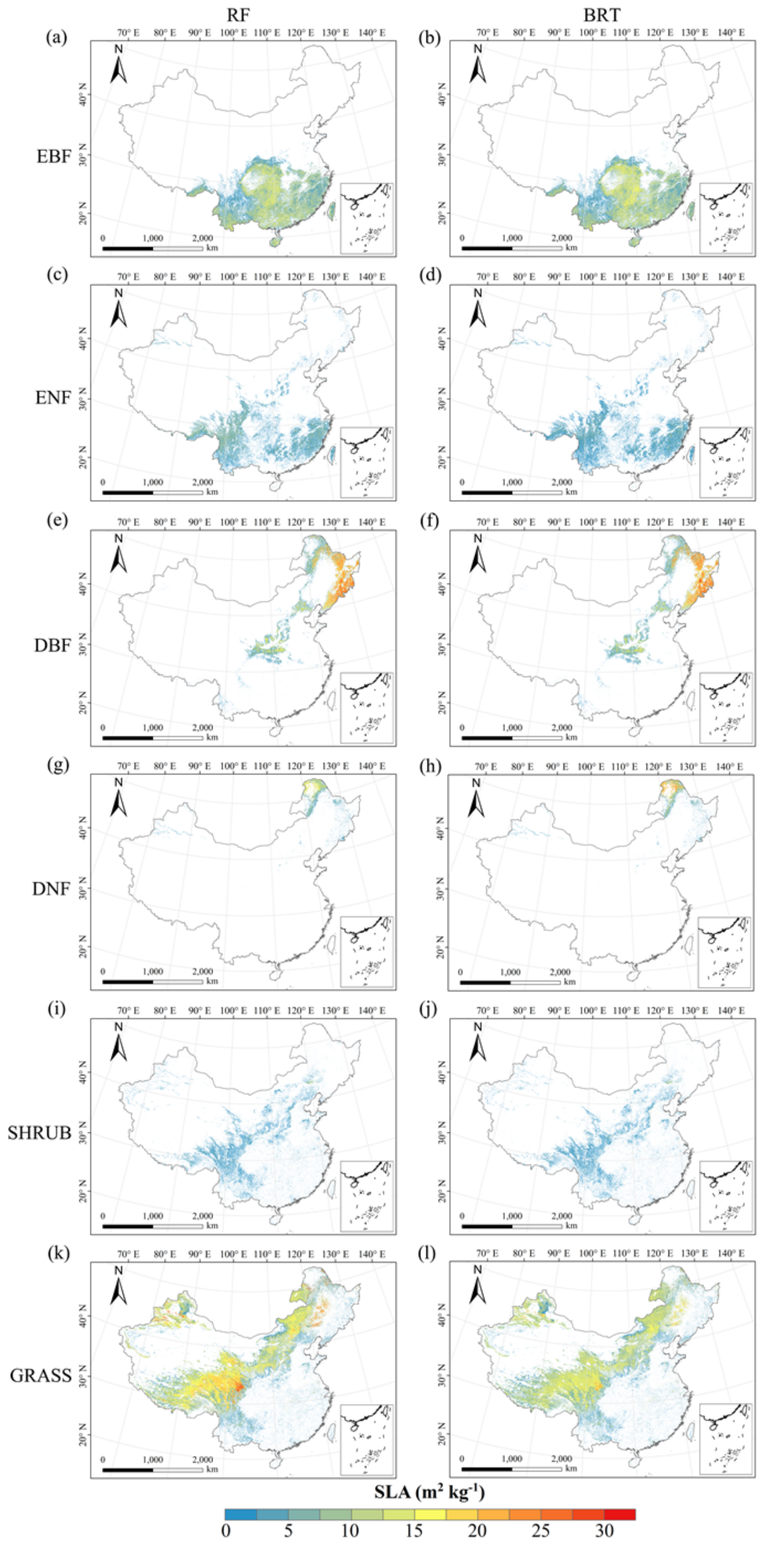

Figure D3. Spatial distribution of specific leaf area (SLA) for each plant functional type. The left penal is obtained from RF (random forest) method, the right penal is obtained from BRT (boosted regression trees) method. The white areas represent other natural vegetation types and artificial land cover types. EBF, evergreen broadleaf forest; ENF, evergreen needleleaf forest; DBF, deciduous broadleaf forest; DNF, deciduous needleleaf forest; SHRUB, shrubland; GRASS, grassland.

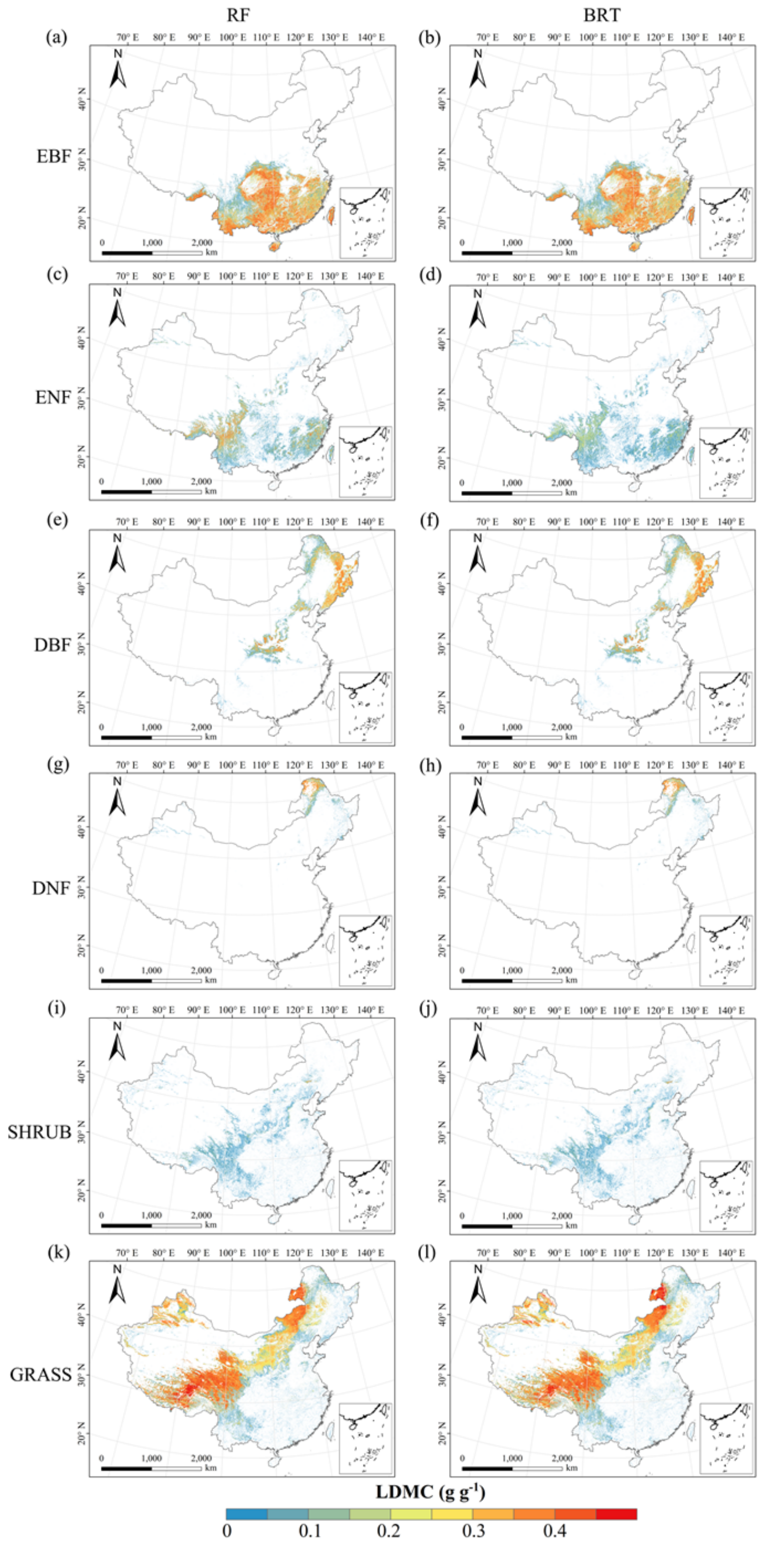

Figure D4. Spatial distribution of leaf dry matter content (LDMC) for each plant functional type. The left penal is obtained from RF (random forest) method, the right penal is obtained from BRT (boosted regression trees) method. The white areas represent other natural vegetation types and artificial land cover types. EBF, evergreen broadleaf forest; ENF, evergreen needleleaf forest; DBF, deciduous broadleaf forest; DNF, deciduous needleleaf forest; SHRUB, shrubland; GRASS, grassland.

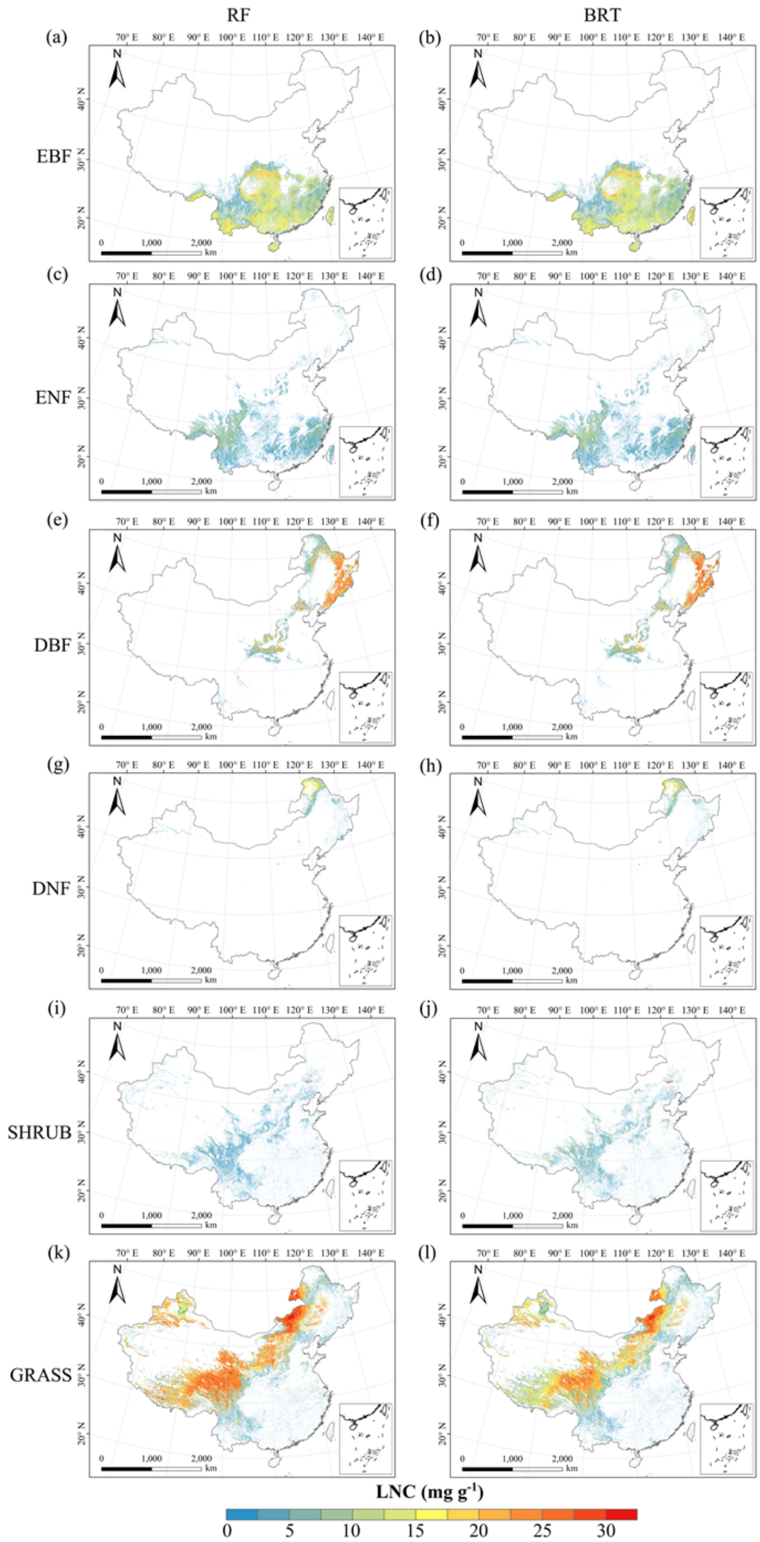

Figure D5. Spatial distribution of leaf N concentration (LNC) for each plant functional type. The left penal is obtained from RF (random forest) method, the right penal is obtained from BRT (boosted regression trees) method. The white areas represent other natural vegetation types and artificial land cover types. EBF, evergreen broadleaf forest; ENF, evergreen needleleaf forest; DBF, deciduous broadleaf forest; DNF, deciduous needleleaf forest; SHRUB, shrubland; GRASS, grassland.

956

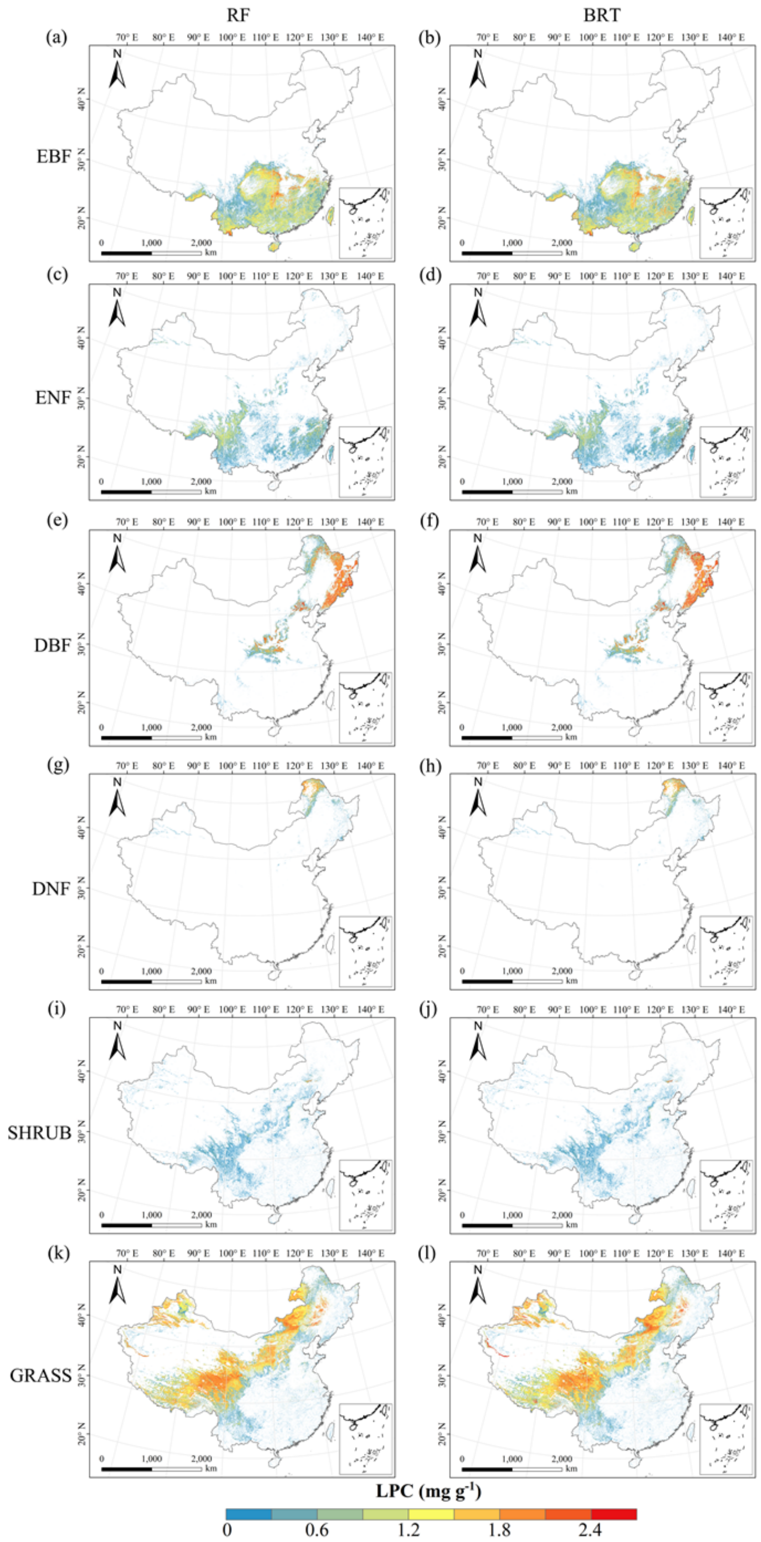

957 **Figure D6.** Spatial distribution of leaf P concentration (LPC) for each plant functional type. The
958 left penal is obtained from RF (random forest) method, the right penal is obtained from BRT
959 (boosted regression trees) method. The white areas represent other natural vegetation types and
960 artificial land cover types. EBF, evergreen broadleaf forest; ENF, evergreen needleleaf forest; DBF,
961 deciduous broadleaf forest; DNF, deciduous needleleaf forest; SHRUB, shrubland; GRASS,
962 grassland.

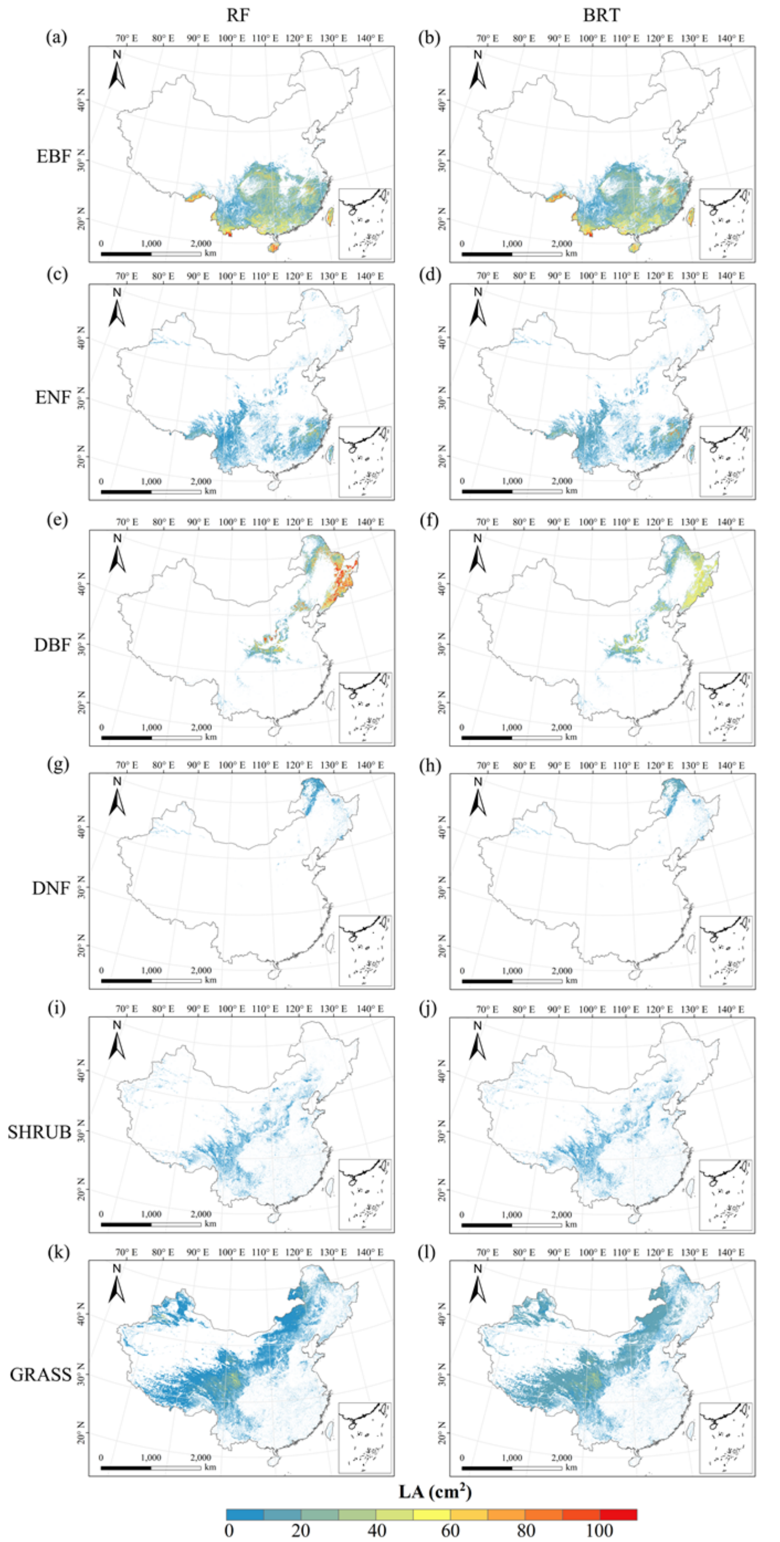

Figure D7. Spatial distribution of leaf area (LA) for each plant functional type. The left penal is obtained from RF (random forest) method, the right penal is obtained from BRT (boosted regression trees) method. The white areas represent other natural vegetation types and artificial land cover types. EBF, evergreen broadleaf forest; ENF, evergreen needleleaf forest; DBF, deciduous broadleaf forest; DNF, deciduous needleleaf forest; SHRUB, shrubland; GRASS, grassland.

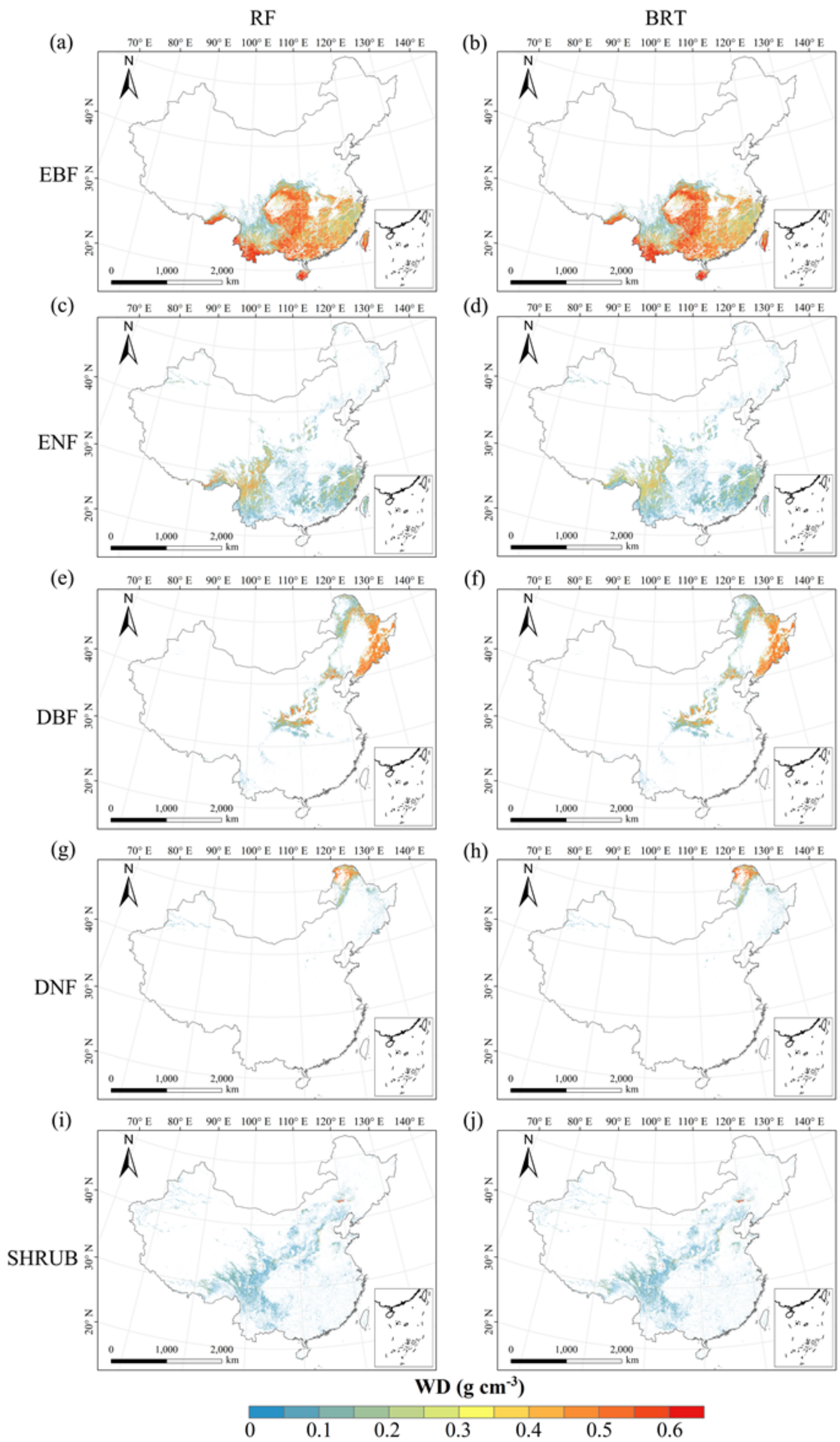

970

971 **Figure D8.** Spatial distribution of wood density (WD) for each plant functional type. The left
972 penal is obtained from RF (random forest) method, the right penal is obtained from BRT (boosted
973 regression trees) method. The white areas represent other natural vegetation types and artificial
974 land cover types. EBF, evergreen broadleaf forest; ENF, evergreen needleleaf forest; DBF,
975 deciduous broadleaf forest; DNF, deciduous needleleaf forest; SHRUB, shrubland.

Appendix E

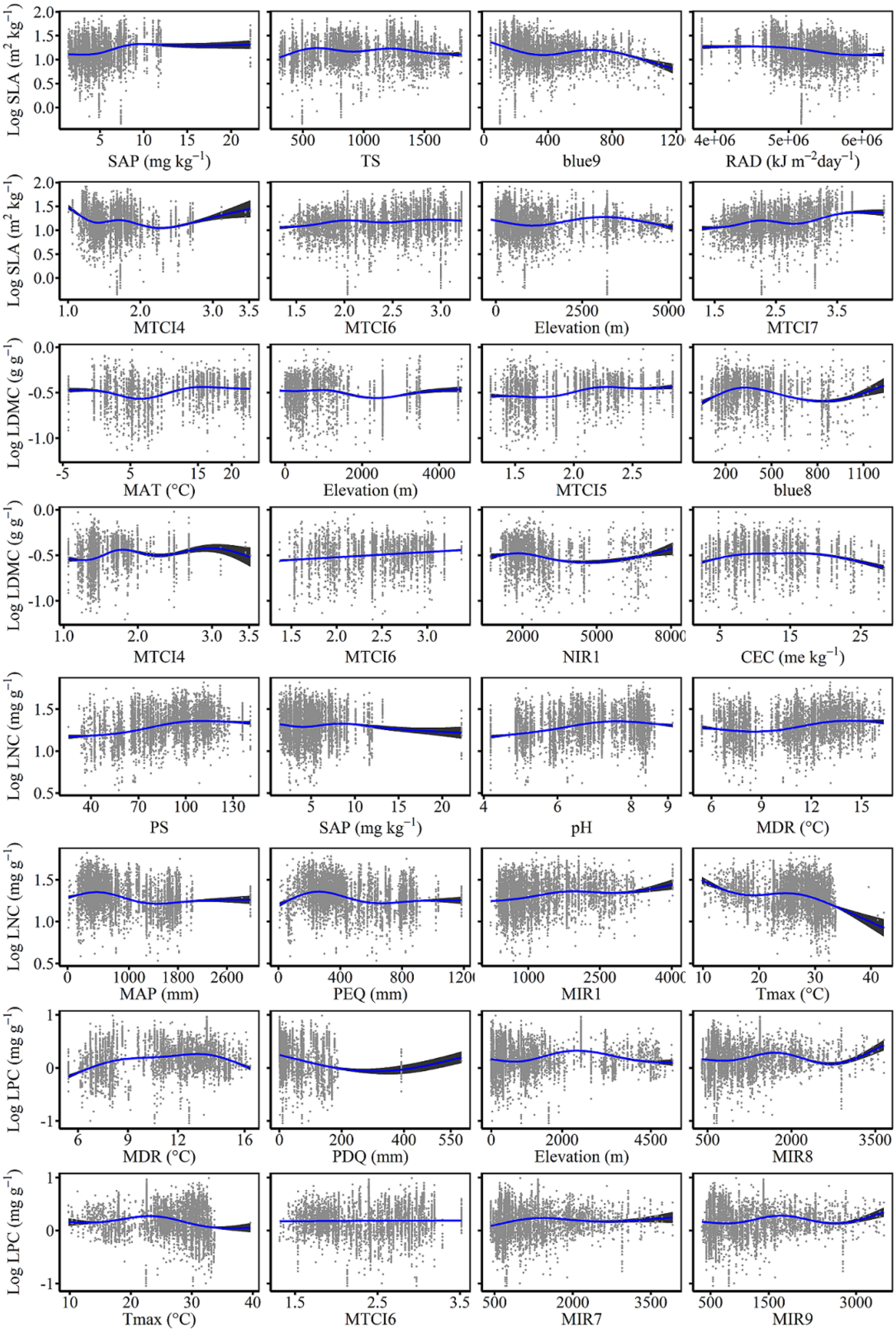

Figure E1. The relationships between SLA (specific leaf area), LDMC (leaf dry matter content), LNC (leaf N concentration), LPC (leaf P concentration) and their eight most important predictors.

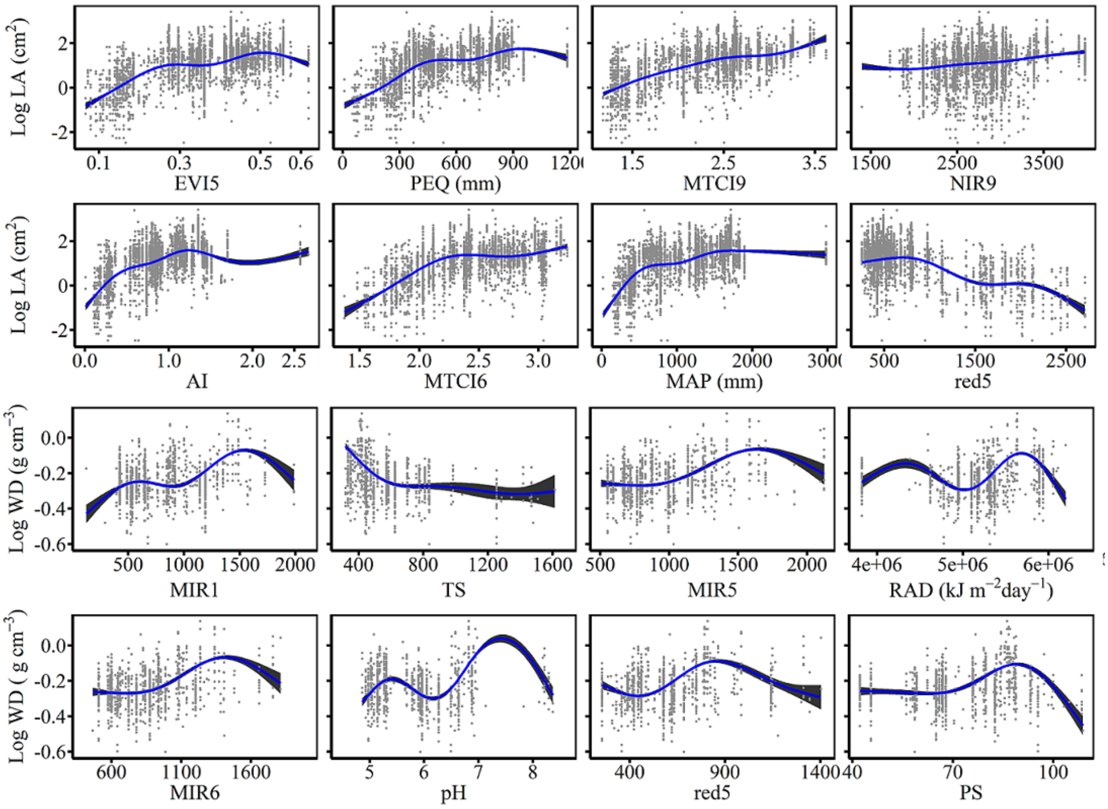

Figure E2. The relationships between LA (leaf area), WD (wood density) and their eight most important predictors.

Appendix F Comparisons between our study with trait maps from previous studies

Given that the trait maps predicted for China were not available from the literature and their authors, we compared our study with those studies performed at the global scale (Table F1). Thus, we extracted the data in China from global trait maps. Before the quantitative comparisons with previous studies, we performed two steps to make the data products as comparable as possible and improve the consistency between different studies. First, due to different spatial resolution of global trait maps (mainly 0.5°) and our study, we resampled the data products of previous studies and our maps to 0.5° spatial resolution. In addition, Vallicrosa et al. (2022) generated the global maps of LNC and LPC with a 1 km spatial resolution, we also compared the frequency distribution of Vallicrosa et al. (2022) with that of our study at a 1 km spatial resolution. Second, our study focused on natural vegetation, so the global trait maps were used to filter out non-natural vegetation (e.g., croplands). For example, Madani et al. (2018) predicted the spatial distribution of SLA that included croplands. We quantitatively compared our maps with previous studies from two perspectives. The comparisons among trait maps were made using frequency plots and spatial correlation (Fig. 7, Table 4 and Fig. F1 in Appendix F). And the maps of spatial differences between our study and previous studies were displayed as Figs. F2-F6 in Appendix F.

Table F1 Summary of related trait maps of previous studies used in this study.

References	Related traits	Methods	Predictors	Consideration of PFT	Spatial resolution
Dong et al. (2023)	SLA LNC	Optimality models	Climate	Yes	0.5°
Vallicrosa et al. (2022)	LNC LPC	Neural networks	Climate Soil N and P deposition	Yes	0.0083°
Schiller et al. (2021)	SLA LNC LA WD	Convolutional Neural Networks	Climate In-situ RGB images	No	0.5°
Boonman et al. (2020)	SLA LNC WD	Generalized linear model, Generalized additive model, Random forest, Boosted regression trees, Ensemble model	Climate Soil	No	0.5°
Moreno et al. (2018)	SLA LNC LPC	Regularized linear regression, Random forest, Neural	Climate Elevation Reflectance	Yes	0.0045°

	LDMC	networks, Kernel networks			
Madani et al. (2018)	SLA	Generalized additive model	Climate	No	0.5°
Butler et al. (2017)	SLA LNC LPC	Bayesian model	Climate Soil	Yes	0.5°
Bodegom et al. (2014)	SLA WD	Multiple regression analysis	Climate Soil	No	0.5°

The resolutions 0.5°, 0.0083° and 0.0045° correspond to square grid cell sizes of about 50 km, 1 km and 500 m at the equator. PFT, plant functional type; SLA, specific leaf area; LDMC, leaf dry matter content; LNC, leaf N concentration; LPC, leaf P concentration; LA, leaf area; WD, wood density.

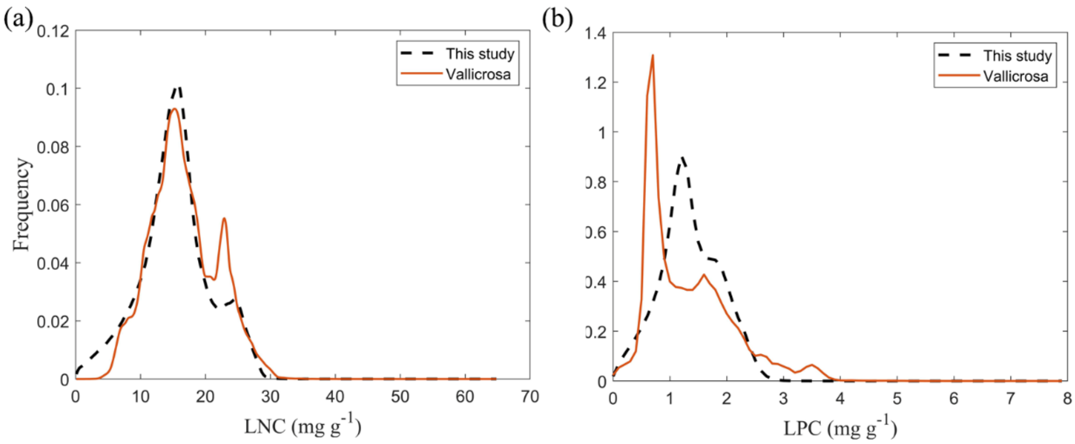

Figure F1. Frequency distributions of plant functional traits in our study ("This study", dashed black lines) and Vallicrosa et al. (2022) at 1 km spatial resolution. (a) LNC, leaf N concentration (mg g^{-1}); (b) LPC, leaf P concentration (mg g^{-1}).

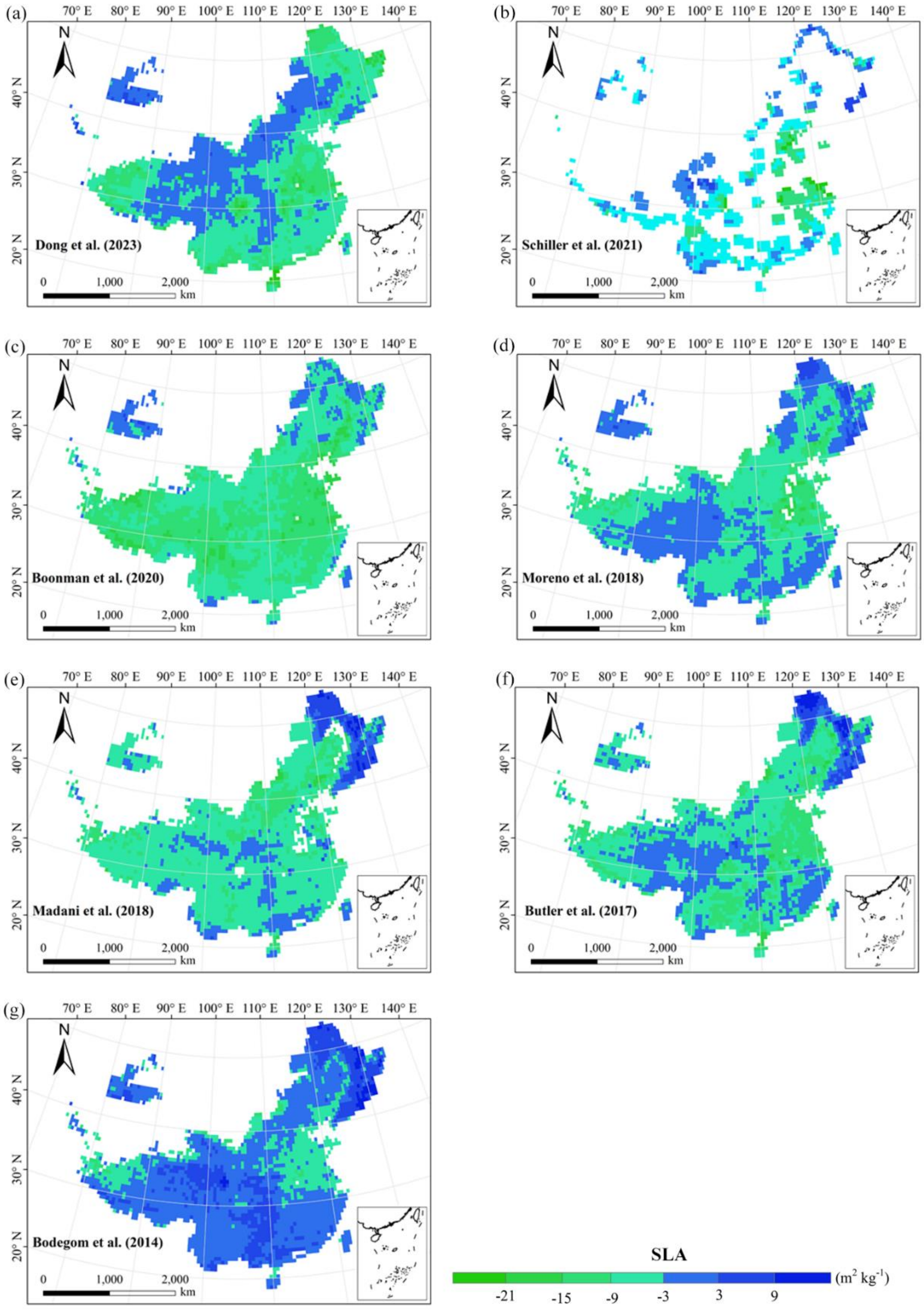

Figure F2. Spatial differences in SLA (specific leaf area, m^2 kg^{-1}) between our study and trait maps from previous studies (see Table F1 for citations).

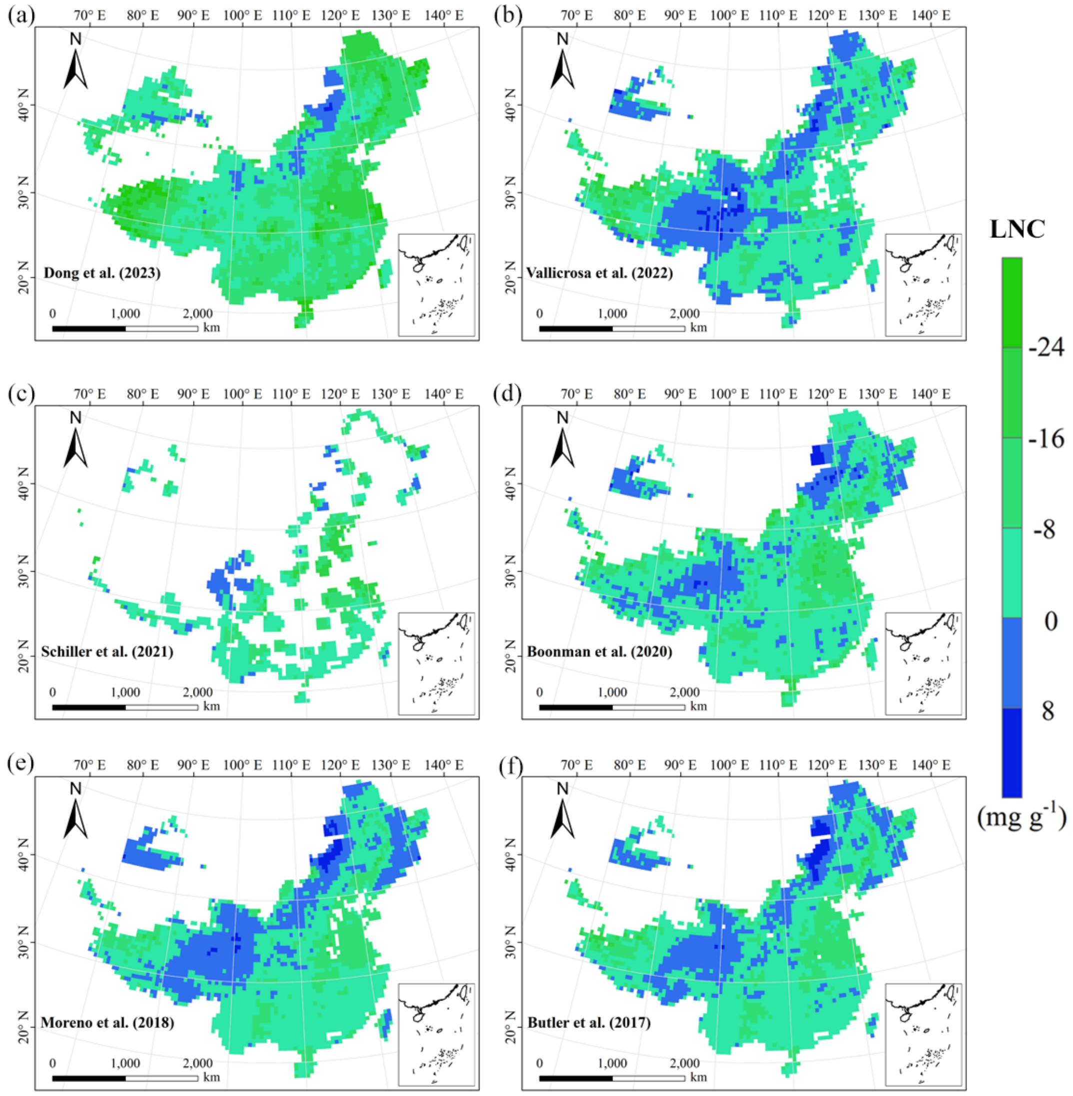

Figure F3. Spatial differences in LNC (leaf N concentration, mg g^{-1}) between our study and trait maps from previous studies (see Table F1 for citations).

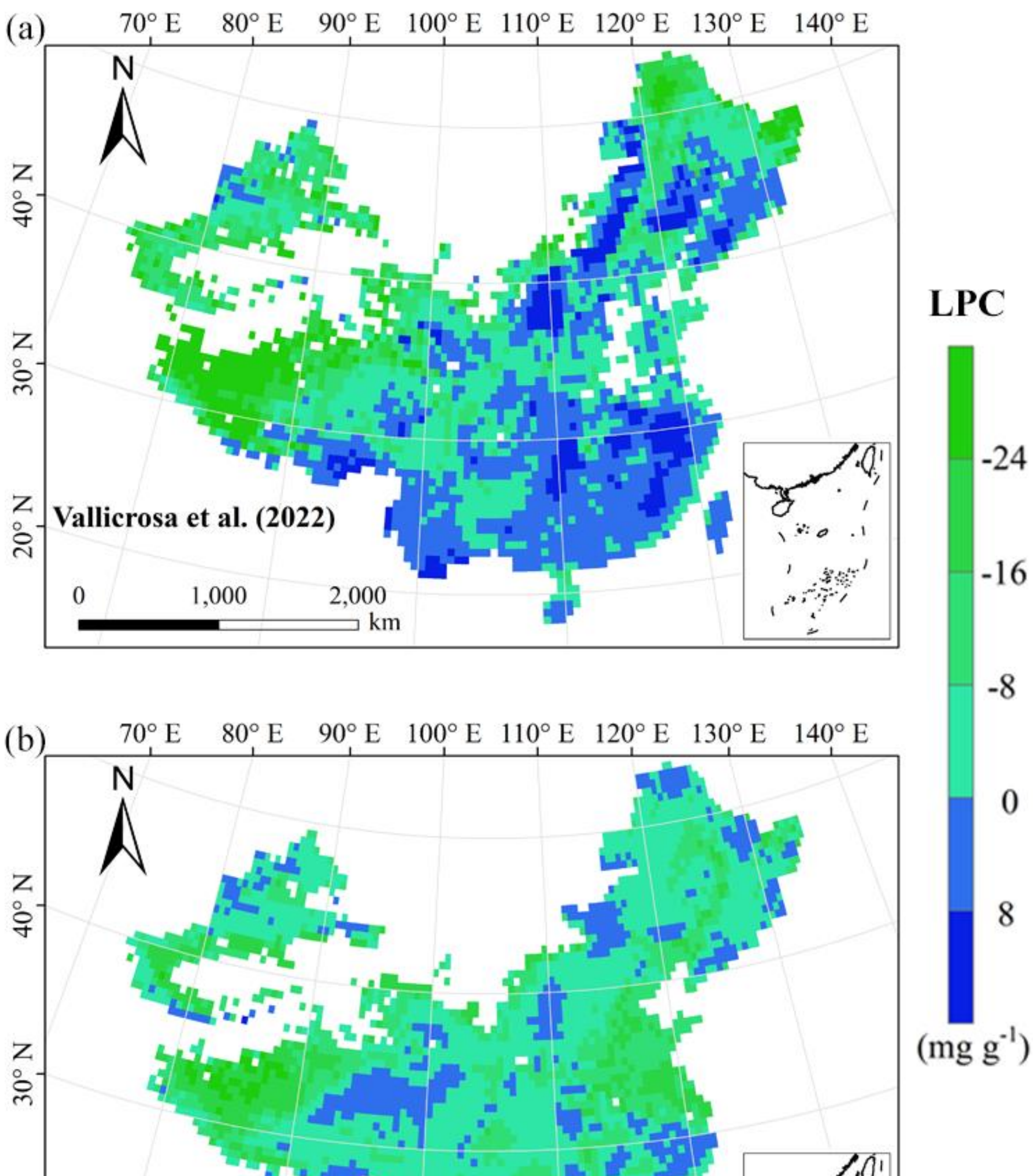

1015

1016 **Figure F4.** Spatial differences in LPC (leaf P concentration, mg g^{-1}) between our study and trait

1017 maps from previous studies (see Table F1 for citations).

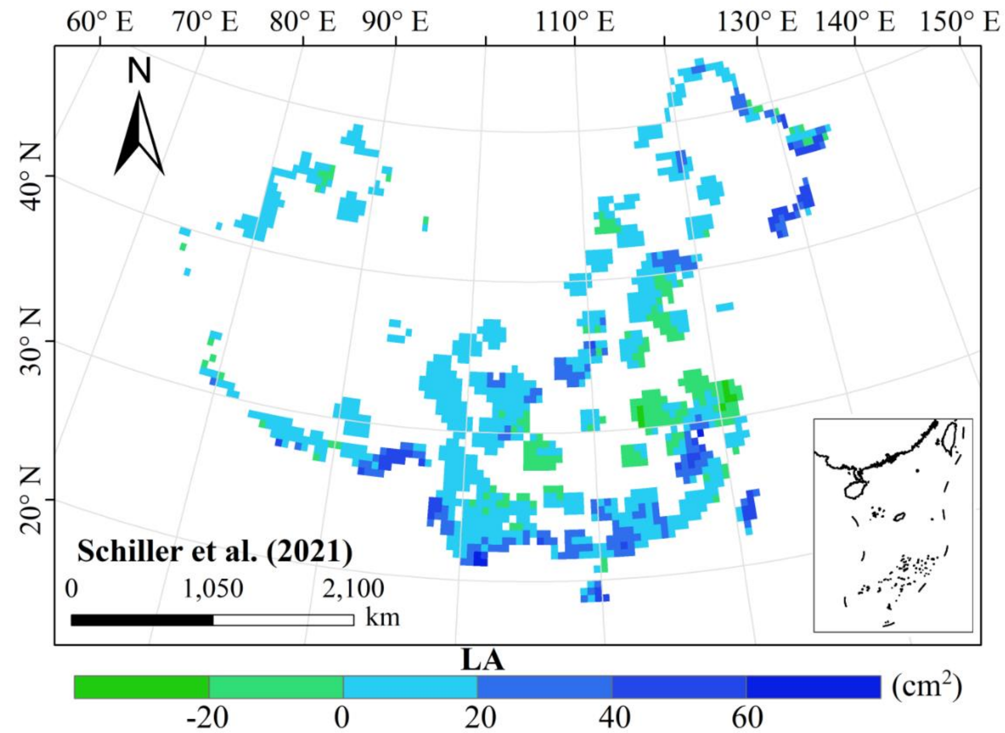

Figure F5. Spatial differences in LA (leaf area, cm^2) between our study and trait maps from previous studies (see Table F1 for citations).

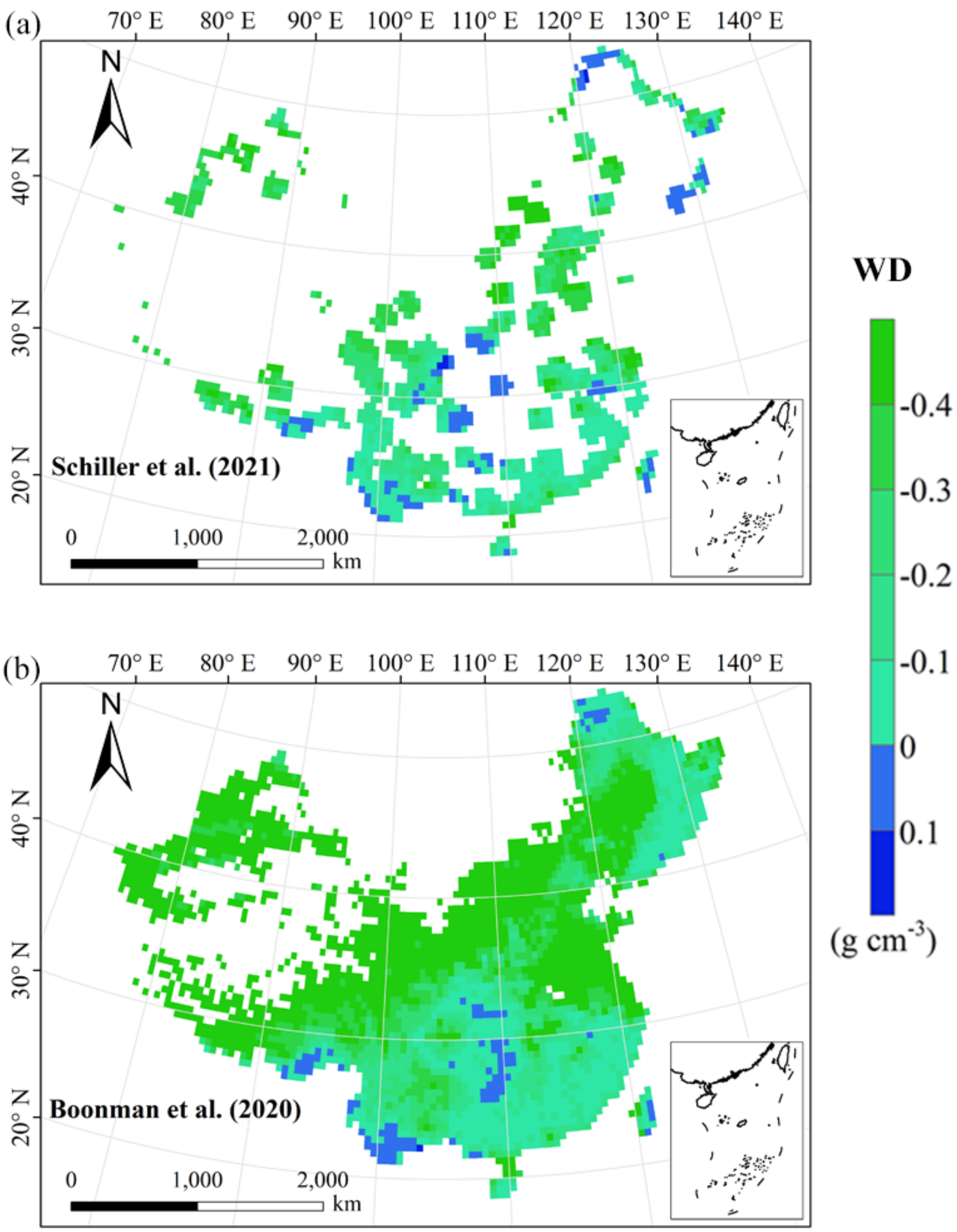

Figure F6. Spatial differences in WD (wood density, g cm^{-3}) between our study and trait maps from previous studies (see Table F1 for citations).

Author contributions. NA and NL designed the research. NA did the analysis, processed the data and wrote the draft of the paper. All co-authors commented on the manuscript and agreed upon the final version of the paper.

Competing interests. The contact author has declared that none of the authors has any competing interests.

Disclaimer. Publisher's note: Copernicus Publications remains neutral with regard to jurisdictional claims in published maps and institutional affiliations.

Acknowledgement. We acknowledge financial supports from the National Natural Science Foundation of China (41991234) and the Joint CAS-MPG Research Project (HZXM20225001MI).

Financial support. This work has been supported by the National Natural Science Foundation of China (grant no. 41991234) and the Joint CAS-MPG Research Project (grant no. HZXM20225001MI).

References

Ali, A. M., Darvishzadeh, R., Skidmore, A. K., van Duren, I., Heiden, U., and Heurich, M.: Estimating leaf functional traits by inversion of PROSPECT: Assessing leaf dry matter content and specific leaf area in mixed mountainous forest. Int. J. Appl. Earth Obs. Geoinf., 45, 66–76, https://doi.org/10.1016/j.jag.2015.11.004, 2016.

An, N. N., Lu, N., Fu, B. J., Wang, M. Y., and He, N. P.: Distinct responses of leaf traits to environment and phylogeny between herbaceous and woody angiosperm species in China. Front. Plant Sci., 12, 799401, https://doi.org/10.3389/fpls.2021.799401, 2021.

Bakker, M. A., Carreño-Rocabado, G., and Poorter, L.: Leaf economics traits predict litter decomposition of tropical plants and differ among land use types. Funct. Ecol., 25, 473–483, https://doi.org/10.1111/j.1365-2435.2010.01802.x, 2011.

Berzaghi, F., Wright, I. J., Kramer, K., Oddou-Muratorio, S., Bohn, F. J., Reyer, C. P. O., Sabate, S., Sanders, T. G. M., and Hartig, F.: Towards a new generation of trait-flexible vegetation models. Trends Ecol. Evol., 35, 191–205, https://doi.org/10.1016/j.tree.2019.11.006, 2020.

Blumenthal, D. M., Mueller, K. E., Kray, J. A., Ocheltree, T. W., Augustine, D. J., Wilcox, K. R., and Cornelissen, H.: Traits link drought resistance with herbivore defence and plant economics in semi-arid grasslands: The central roles of phenology and leaf dry matter content. J. Ecol., 108, 2336–2351, https://doi.org/10.1111/1365-2745.13454, 2020.

Bohner, A. Soil chemical properties as indicators of plant species richness in grassland communities. Integrating efficient grassland farming and biodiversity, Proceedings of the 13th International Occasional Symposium of the European Grassland Federation, Tartu, Estonia, 29–31 August, 48-51, 2005.

Boonman, C. C. F., Benitez-Lopez, A., Schipper, A. M., Thuiller, W., Anand, M., Cerabolini, B. E. L., Cornelissen, J. H. C., Gonzalez-Melo, A., Hattingh, W. N., Higuchi, P., Laughlin, D. C., Onipchenko, V. G., Penuelas, J., Poorter, L., Soudzilovskaia, N. A., Huijbregts, M. A. J., and Santini, L.: Assessing the reliability of predicted plant trait distributions at the global scale. Global Ecol. Biogeogr., 29, 1034–1051, https://doi.org/10.1111/geb.13086, 2020.

Breiman, L.: Random forests. Mach. Learn., 45, 5–32, https://doi.org/10.1023/a:1010933404324, 2001.

Bruelheide, H., Dengler, J., Purschke, O., Lenoir, J., Jimenez-Alfaro, B., Hennekens, S. M., Botta-Dukat, Z., Chytry, M., Field, R., Jansen, F., Kattge, J., Pillar, V. D., Schrodt, F., Mahecha, M. D., Peet, R. K., Sandel, B., van Bodegom, P., Altman, J., Alvarez-Davila, E., Arfin Khan, M. A. S., et al.: Global trait-environment relationships of plant communities. Nat. Ecol. Evol., 2, 1906–1917, https://doi.org/10.1038/s41559-018-0699-8, 2018.

Bruelheide, H., Dengler, J., Jiménez‐Alfaro, B., Purschke, O., Hennekens, S. M., Chytrý, M., Pillar, V. D., Jansen, F., Kattge, J., Sandel, B., Aubin, I., Biurrun, I., Field, R., Haider, S., Jandt, U., Lenoir, J., Peet, R. K., Peyre, G., Sabatini, F. M., Schmidt, M., et al.: sPlot – A new tool for global vegetation analyses. J. Veg. Sci., 30, 161–186, https://doi.org/10.1111/jvs.12710, 2019.

Buchhorn, M., Bertels, L., Smets, B., De Roo, B., Lesiv, M., Tsendbazar, N. E., Masiliunas, D., and Linlin, L.: Copernicus Global Land Service: Land Cover 100m: Version 3 Globe 2015-2019: Algorithm Theoretical Basis Document. https://doi.org/10.5281/zenodo.3938968, 2020.

Butler, E. E., Datta, A., Flores-Moreno, H., Chen, M., Wythers, K. R., Fazayeli, F., Banerjee, A., Atkin, O. K., Kattge, J., Amiaud, B., Blonder, B., Boenisch, G., Bond-Lamberty, B., Brown, K. A., Byun, C., Campetella, G., Cerabolini, B. E. L., Cornelissen, J. H. C., Craine, J. M., Craven, D., de Vries, F. T., Diaz, S., Domingues, T. F., Forey, E., Gonzalez-Melo, A., Gross, N., Han, W., Hattingh, W. N., Hickler, T., Jansen, S., Kramer, K., Kraft, N. J. B., Kurokawa, H., Laughlin, D. C., Meir, P., Minden, V., Niinemets, U., Onoda, Y., Penuelas, J., Read, Q., Sack, L., Schamp, B., Soudzilovskaia, N. A., Spasojevic, M. J., Sosinski, E., Thornton, P. E., Valladares, F., van Bodegom, P. M., Williams, M., Wirth, C., and Reich, P. B.: Mapping local and global variability in plant trait distributions. P. Natl. Acad. Sci. USA, 114, 10937–10946, https://doi.org/10.1073/pnas.1708984114, 2017.

Cavender-Bares, J., Schneider, F. D., Santos, M. J., Armstrong, A., Carnaval, A., Dahlin, K. M., Fatoyinbo, L., Hurtt, G. C., Schimel, D., Townsend, P. A., Ustin, S. L., Wang, Z. H., and Wilson, A. M.: Integrating remote sensing with ecology and evolution to advance biodiversity conservation. Nat. Ecol. Evol., 6, 506–519, https://doi.org/10.1038/s41559-022-01702-5, 2022.

Clevers, J. G. P. W., and Gitelson, A. A.: Remote estimation of crop and grass chlorophyll and nitrogen content using red-edge bands on Sentinel-2 and -3. Int. J. Appl. Earth Obs. Geoinf., 23, 344–351, https://doi.org/10.1016/j.jag.2012.10.008, 2013.

Dahlin, K. M., Asner, G. P., and Field, C. B.: Environmental and community controls on plant canopy chemistry in a Mediterranean-type ecosystem. P. Natl. Acad. Sci. USA, 110, 6895–6900, https://doi.org/10.1073/pnas.1215513110, 2013.

Darvishzadeh, R., Skidmore, A., Schlerf, M., and Atzberger, C.: Inversion of a radiative transfer model for estimating vegetation LAI and chlorophyll in a heterogeneous grassland. Remote Sens. Environ., 112, 2592–2604, https://doi.org/10.1016/j.rse.2007.12.003, 2008.

Diaz, S., Kattge, J., Cornelissen, J. H., Wright, I. J., Lavorel, S., Dray, S., Reu, B., Kleyer, M., Wirth, C., Prentice, I. C., Garnier, E., Bonisch, G., Westoby, M., Poorter, H., Reich, P. B., Moles, A. T., Dickie, J., Gillison, A. N., Zanne, A. E., Chave, J., Wright, S. J., Sheremet'ev, S. N., Jactel, H., Baraloto, C., Cerabolini, B., Pierce, S., Shipley, B., Kirkup, D., Casanoves, F., Joswig, J. S., Gunther, A., Falczuk, V., Ruger, N., Mahecha, M. D., and Gorne, L. D.: The global spectrum of plant form and function. Nature, 529, 167–171, https://doi.org/10.1038/nature16489, 2016.

Diaz, S., Hodgson, J. G., Thompson, K., Cabido, M., Cornelissen, J. H. C., Jalili, A., Montserrat-Marti, G., Grime, J. P., Zarrinkamar, F., Asri, Y., Band, S. R., Basconcelo, S., Castro-Diez, P., Funes, G., Hamzehee, B., Khoshnevi, M., Perez-Harguindeguy, N., Perez-Rontome, M. C., Shirvany, F. A., Vendramini, F., Yazdani, S., Abbas-Azimi, R., Bogaard, A., Boustani, S., Charles, M., Dehghan, M., de Torres-Espuny, L., Falczuk, V., Guerrero-Campo, J., Hynd, A., Jones, G., Kowsary, E., Kazemi-Saeed, F., Maestro-Martinez, M., Romo-Diez, A., Shaw, S., Siavash, B., Villar-Salvador, P., and Zak, M. R.: The plant traits that drive ecosystems: Evidence from three continents. J. Veg. Sci., 15, 295–304, https://doi.org/10.1111/j.1654-1103.2004.tb02266.x, 2004.

Dong, N., Dechant, B., Wang, H., Wright, I. J., and Prentice, IC.: Global leaf-trait mapping based on optimality theory. Global Ecol. Biogeogr., 32, 1152–1162, https://doi.org/10.1111/geb.13680, 2023.

Du, L., Liu, H., Guan, W., Li, J., and Li, J.: Drought affects the coordination of belowground and aboveground resource-related traits in *Solidago canadensis* in China. Ecol. Evol., 9, 9948–9960, https://doi.org/10.1002/ece3.5536, 2019.

Elith, J., Leathwick, J. R., and Hastie, T.: A working guide to boosted regression trees. J. Anim. Ecol., 77, 802–813, https://doi.org/10.1111/j.1365-2656.2008.01390.x, 2008.

Elith, J., Kearney, M., and Phillips, S.: The art of modelling range-shifting species. Methods Ecol. Evol., 1, 330–342, https://doi.org/10.1111/j.2041-210X.2010.00036.x, 2010.

Elith, J., Graham, C. H., Anderson, R. P., Dudik, M., Ferrier, S., Guisan, A., Hijmans, R. J., Huettmann, F., Leathwick, J. R., Lehmann, A., Li, J., Lohmann, L. G., Loiselle, B. A., Manion, G., Moritz, C., Nakamura, M., Nakazawa, Y., Overton, J. M., Peterson, A. T., Phillips, S. J., Richardson, K., Scachetti-Pereira, R., Schapire, R. E., Soberon, J., Williams, S., Wisz, M. S., and Zimmermann, N. E.: Novel methods improve prediction of species' distributions from occurrence data. Ecography, 29, 129–151, https://doi.org/10.1111/j.2006.0906-7590.04596.x, 2006.

Finzi, A. C., Austin, A. T., Cleland, E. E., Frey, S. D., Houlton, B. Z., and Wallenstein, M. D.: Responses and feedbacks of coupled biogeochemical cycles to climate change: examples from terrestrial ecosystems. Front. Ecol. Environ., 9, 61–67, https://doi.org/10.1890/100001, 2011.

Foley, J. A., Prentice, I. C., Ramankutty, N., Levis, S., Pollard, D., Sitch, S., and Haxeltine, A.: An integrated biosphere model of land surface processes, terrestrial carbon balance, and vegetation dynamics. Global Biogeochem. Cy., 10, 603–628, https://doi.org/10.1029/96gb02692, 1996.

Freschet, G. T., Cornelissen, J. H. C., van Logtestijn, R. S. P., and Aerts, R.: Evidence of the ‘plant economics spectrum’ in a subarctic flora. J. Ecol., 98, 362–373, https://doi.org/10.1111/j.1365-2745.2009.01615.x, 2010.

Grime, J. P.: Benefits of plant diversity to ecosystems: immediate, filter and founder effects. J. Ecol., 86, 902–910, https://doi.org/10.1046/j.1365-2745.1998.00306.x, 1998.

He, N. P., Yan, P., Liu, C. C., Xu, L., Li, M. X., Van Meerbeek, K., Zhou, G. S., Zhou, G. Y., Liu, S. R., Zhou, X. H., Li, S. G., Niu, S. L., Han, X. G., Buckley, T. N., Sack, L., and Yu, G. R.: Predicting ecosystem productivity based on plant community traits. Trends Plant Sci., 28, 43–53, https://doi.org/10.1016/j.tplants.2022.08.015, 2023.

Hodgson, J. G., Montserrat-Marti, G., Charles, M., Jones, G., Wilson, P., Shipley, B., Sharafi, M., Cerabolini, B. E. L., Cornelissen, J. H. C., Band, S. R., Bogard, A., Castro-Diez, P., Guerrero-Campo, J., Palmer, C., Perez-Rontome, M. C., Carter, G., Hynd, A., Romo-Diez, A., Espuny, L. D., and Pla, F. R.: Is leaf dry matter content a better predictor of soil fertility than specific leaf area? Ann. Bot., 108, 1337–1345, https://doi.org/10.1093/aob/mcr225, 2011.

Hoeber, S., Leuschner, C., Köhler, L., Arias-Aguilar, D., and Schuldt, B.: The importance of hydraulic conductivity and wood density to growth performance in eight tree species from a tropical semi-dry climate. Forest Ecol. Manag., 330, 126–136, https://doi.org/10.1016/j.foreco.2014.06.039, 2014.

Jónsdóttir, I. S., Halbritter, A. H., Christiansen, C. T., Althuizen, I. H. J., Haugum, S. V., Henn, J. J., Björnsdóttir, K., Maitner, B. S., Malhi, Y., Michaletz, S. T., Roos, R. E., Klanderud, K., Lee, H., Enquist, B. J., and Vandvik, V.: Intraspecific trait variability is a key feature underlying high Arctic plant community resistance to climate warming. Ecol. Monogr., 93, e1555, https://doi.org/10.1002/ecm.1555, 2022.

Jung, V., Violle, C., Mondy, C., Hoffmann, L., and Muller, S.: Intraspecific variability and trait-based community assembly. J. Ecol., 98, 1134–1140, https://doi.org/10.1111/j.1365-2745.2010.01687.x, 2010.

Kattge, J., Diaz, S., Lavorel, S., Prentice, C., Leadley, P., Bonisch, G., Garnier, E., Westoby, M., Reich, P. B., Wright, I. J., Cornelissen, J. H. C., Violle, C., Harrison, S. P., van Bodegom, P.

M., Reichstein, M., Enquist, B. J., Soudzilovskaia, N. A., Ackerly, D. D., Anand, M., Atkin, O., et al.: TRY - A global database of plant traits. Global Change Biol., 17, 2905–2935, https://doi.org/10.1111/j.1365-2486.2011.02451.x, 2011.

Kattge, J., Bonisch, G., Diaz, S., Lavorel, S., Prentice, I. C., Leadley, P., Tautenhahn, S., Werner, G. D. A., Aakala, T., Abedi, M., Acosta, A. T. R., Adamidis, G. C., Adamson, K., Aiba, M., Albert, C. H., Alcantara, J. M., Alcazar, C. C., Aleixo, I., Ali, H., Amiaud, B., et al.: TRY plant trait database - Enhanced coverage and open access. Global Change Biol., 26, 119–188, https://doi.org/10.1111/gcb.14904, 2020.

King, D. A., Davies, S. J., Tan, S., and Noor, N. S. M.: The role of wood density and stem support costs in the growth and mortality of tropical trees. J. Ecol., 94, 670–680, https://doi.org/10.1111/j.1365-2745.2006.01112.x, 2006.

Kirilenko, A. P., Belotelov, N. V., and Bogatyrev, B. G.: Global model of vegetation migration: incorporation of climatic variability. Ecol. Model., 132, 125–133, https://doi.org/10.1016/S0304-3800(00)00310-0, 2000.

LeBauer, D. S., and Treseder, K. K.: Nitrogen limitation of net primary productivity in terrestrial ecosystems is globally distributed. Ecology, 89, 371–379, https://doi.org/10.1890/06-2057.1, 2008.

Li, C. X., Wulf, H., Schmid, B., He, J. S., and Schaepman, M. E.: Estimating plant traits of alpine grasslands on the Qinghai-Tibetan Plateau using remote sensing. IEEE J. Sel. Top. Appl. Earth Obs. Remote Sens., 11, 2263–2275, https://doi.org/10.1109/jstars.2018.2824901, 2018.

Li, D. J., Ives, A. R., and Waller, D. M.: Can functional traits account for phylogenetic signal in community composition? New Phytol., 214, 607–618, https://doi.org/10.1111/nph.14397, 2017.

Li, Y. Q., Reich, P. B., Schmid, B., Shrestha, N., Feng, X., Lyu, T., Maitner, B. S., Xu, X., Li, Y. C., Zou, D. T., Tan, Z. H., Su, X. Y., Tang, Z. Y., Guo, Q. H., Feng, X. J., Enquist, B. J., and Wang, Z. H.: Leaf size of woody dicots predicts ecosystem primary productivity. Ecol. Lett., 23, 1003–1013, https://doi.org/10.1111/ele.13503, 2020.

Liang, X. Y., Ye, Q., Liu, H., and Brodribb, T. J.: Wood density predicts mortality threshold for diverse trees. New Phytol., 229, 3053–3057, https://doi.org/10.1111/nph.17117, 2021.

Liaw, A., and Wiener, M.: Classification and Regression by randomForest. R News, 2, 18–22, 2002.

Liu, H. Y., and Yin, Y.: Response of forest distribution to past climate change: an insight into future predictions. Chinese Sci. Bull., 58, 4426–4436, https://doi.org/10.1007/s11434-013-6032-7, 2013.

Loozen, Y., Rebel, K. T., Karssenberg, D., Wassen, M. J., Sardans, J., Peñuelas, J., and De Jong, S. M.: Remote sensing of canopy nitrogen at regional scale in Mediterranean forests using the spaceborne MERIS Terrestrial Chlorophyll Index. Biogeosciences, 15, 2723–2742, https://doi.org/10.5194/bg-15-2723-2018, 2018.

Loozen, Y., Rebel, K. T., de Jong, S. M., Lu, M., Ollinger, S. V., Wassen, M. J., and Karssenberg, D.: Mapping canopy nitrogen in European forests using remote sensing and environmental variables with the random forests method. Remote Sens. Environ., 247, 111933, https://doi.org/10.1016/j.rse.2020.111933, 2020.

Madani, N., Kimball, J. S., Ballantyne, A. P., Affleck, D. L. R., van Bodegom, P. M., Reich, P. B., Kattge, J., Sala, A., Nazeri, M., Jones, M. O., Zhao, M., and Running, S. W.: Future global productivity will be affected by plant trait response to climate. Sci. Rep., 8, 1–10, https://doi.org/10.1038/s41598-018-21172-9, 2018.

Martínez-Vilalta, J., Mencuccini, M., Vayreda, J., and Retana, J.: Interspecific variation in functional traits, not climatic differences among species ranges, determines demographic rates across 44 temperate and Mediterranean tree species. J. Ecol., 98, 1462–1475, https://doi.org/10.1111/j.1365-2745.2010.01718.x, 2010.

Matheny, A. M., Mirfenderesgi, G., and Bohrer, G.: Trait-based representation of hydrological functional properties of plants in weather and ecosystem models. Plant Divers., 39, 1–12, https://doi.org/10.1016/j.pld.2016.10.001, 2017.

Moreno-Martínez, Á., Camps-Valls, G., Kattge, J., Robinson, N., Reichstein, M., van Bodegom, P., Kramer, K., Cornelissen, J. H. C., Reich, P., Bahn, M., Niinemets, Ü., Peñuelas, J., Craine, J. M., Cerabolini, B. E. L., Minden, V., Laughlin, D. C., Sack, L., Allred, B., Baraloto, C., Byun, C., Soudzilovskaia, N. A., and Running, S. W.: A methodology to derive global maps of leaf traits using remote sensing and climate data. Remote Sens. Environ., 218, 69–88, https://doi.org/10.1016/j.rse.2018.09.006, 2018.

Myers-Smith, I. H., Thomas, H. J. D., and Bjorkman, A. D.: Plant traits inform predictions of tundra responses to global change. New Phytol., 221, 1742–1748, https://doi.org/10.1111/nph.15592, 2019.

NEODC, 2015. NEODC - NERC Earth Observation Data Centre. Natural Environment Research Council. http://neodc.nerc.ac.uk/.

Peng, C. H.: From static biogeographical model to dynamic global vegetation model: a global perspective on modelling vegetation dynamics. Ecol. Model., 135, 33–54, https://doi.org/10.1016/S0304-3800(00)00348-3, 2000.

Perez-Harguindeguy, N., Diaz, S., Garnier, E., Lavorel, S., Poorter, H., Jaureguiberry, P., Bret-Harte, M. S., Cornwell, W. K., Craine, J. M., Gurvich, D. E., Urcelay, C., Veneklaas, E. J., Reich, P. B., Poorter, L., Wright, I. J., Ray, P., Enrico, L., Pausas, J. G., de Vos, A. C., Buchmann, N., Funes, G., Quetier, F., Hodgson, J. G., Thompson, K., Morgan, H. D., ter Steege, H., van der Heijden, M. G. A., Sack, L., Blonder, B., Poschlod, P., Vaieretti, M. V., Conti, G., Staver, A. C., Aquino, S., and Cornelissen, J. H. C.: New handbook for standardised measurement of plant functional traits worldwide. Aust. Bot., 61, 167–234, https://doi.org/10.1071/bt12225, 2013.

Piao, S. L., He, Y., Wang, X. H., and Chen, F. H.: Estimation of China's terrestrial ecosystem carbon sink: Methods, progress and prospects. Sci. China Earth Sci., 65, 641–651, https://doi.org/10.1007/s11430-021-9892-6, 2022.

Qiao, J. J., Zuo, X. A., Yue, P., Wang, S. K., Hu, Y., Guo, X. X., Li, X. Y., Lv, P., Guo, A. X., and Sun, S. S.: High nitrogen addition induces functional trait divergence of plant community in a temperate desert steppe. Plant Soil, 487, 133–156, https://doi.org/10.1007/s11104-023-05910-1, 2023.

Reich, P. B., and Oleksyn, J.: Global patterns of plant leaf N and P in relation to temperature and latitude. P. Natl. Acad. Sci. USA, 101, 11001–11006, https://doi.org/10.1073/pnas.0403588101, 2004.

Reich, P. B., Uhl, C., Waiters, M. B., and Ellsworth, D. S.: Leaf lifespan as a determinant of leaf structure and function among 23 Amazonian tree species. Oeologia, 86, 16–24, https://doi.org/10.1007/BF00317383, 1991.

Ridgeway, G.: Gbm: generalized boosted regression models. R package version 1.5-6, Available at: http://cran.r-project.org/web/packages/gbm/index.html, accessed 11/02/2009, 2006.

Roderick, M. L., and Berry, S. L.: Linking wood density with tree growth and environment: a theoretical analysis based on the motion of water. New Phytol., 149, 473–485, https://doi.org/10.1046/j.1469-8137.2001.00054.x, 2002.

Romero, A., Aguado, I., and Yebra, M.: Estimation of dry matter content in leaves using normalized indexes and PROSPECT model inversion. Int. J. Remote Sens., 33, 396–414, https://doi.org/10.1080/01431161.2010.532819, 2012.

Sakschewski, B., von Bloh, W., Boit, A., Rammig, A., Kattge, J., Poorter, L., Penuelas, J., and Thonicke, K.: Leaf and stem economics spectra drive diversity of functional plant traits in a dynamic global vegetation model. Global Change Biol., 21, 2711–2725, https://doi.org/10.1111/gcb.12870, 2015.

Scheiter, S., Langan, L., and Higgins, S. I.: Next-generation dynamic global vegetation models: learning from community ecology. New Phytol., 198, 957–969, https://doi.org/10.1111/nph.12210, 2013.

Schiller, C., Schmidtlein, S., Boonman, C., Moreno-Martinez, A., and Kattenborn, T.: Deep learning and citizen science enable automated plant trait predictions from photographs. Sci. Rep., 11, 16395, https://doi.org/10.1038/s41598-021-95616-0, 2021.

Shangguan, W., Dai, Y. J., Liu, B. Y., Zhu, A. X., Duan, Q. Y., Wu, L. Z., Ji, D. Y., Ye, A. Z., Yuan, H., Zhang, Q., Chen, D. D., Chen, M., Chu, J. T., Dou, Y. J., Guo, J. X., Li, H. Q., Li, J. J., Liang, L., Liang, X., Liu, H. P., Liu, S. Y., Miao, C. Y., and Zhang, Y. Z.: A China data set of soil properties for land surface modeling. J. Adv. Model. Earth Syst., 5, 212–224, https://doi.org/10.1002/jame.20026, 2013.

Siefert, A., Violle, C., Chalmandrier, L., Albert, C. H., Taudiere, A., Fajardo, A., Aarssen, L. W., Baraloto, C., Carlucci, M. B., Cianciaruso, M. V., de, L. D. V., de Bello, F., Duarte, L. D., Fonseca, C. R., Freschet, G. T., Gaucherand, S., Gross, N., Hikosaka, K., Jackson, B., Jung, V., Kamiyama, C., Katabuchi, M., Kembel, S. W., Kichenin, E., Kraft, N. J., Lagerstrom, A., Bagousse-Pinguet, Y. L., Li, Y., Mason, N., Messier, J., Nakashizuka, T., Overton, J. M., Peltzer, D. A., Perez-Ramos, I. M., Pillar, V. D., Prentice, H. C., Richardson, S., Sasaki, T., Schamp, B. S., Schob, C., Shipley, B., Sundqvist, M., Sykes, M. T., Vandewalle, M., and Wardle, D. A.: A global meta-analysis of the relative extent of intraspecific trait variation in plant communities. Ecol. Lett., 18, 1406–1419, https://doi.org/10.1111/ele.12508, 2015.

Šímová, I., Sandel, B., Enquist, B. J., Michaletz, S. T., Kattge, J., Violle, C., McGill, B. J., Blonder, B., Engemann, K., Peet, R. K., Wiser, S. K., Morueta-Holme, N., Boyle, B., Kraft, N. J. B., Svenning, J. C., and Hector, A.: The relationship of woody plant size and leaf nutrient content to large-scale productivity for forests across the Americas. J. Ecol., 107, 2278–2290, https://doi.org/10.1111/1365-2745.13163, 2019.

Sitch, S., Huntingford, C., Gedney, N., Levy, P. E., Lomas, M., Piao, S. L., Betts, R., Ciais, P., Cox, P., Friedlingstein, P., Jones, C. D., Prentice, I. C., and Woodward, F. I.: Evaluation of the terrestrial carbon cycle, future plant geography and climate-carbon cycle feedbacks using five Dynamic Global Vegetation Models (DGVMs). Global Change Biol., 14, 2015–2039, https://doi.org/10.1111/j.1365-2486.2008.01626.x, 2008.

Smart, S. M., Glanville, H. C., Blanes, M. d. C., Mercado, L. M., Emmett, B. A., Jones, D. L., Cosby, B. J., Marrs, R. H., Butler, A., Marshall, M. R., Reinsch, S., Herrero-Jáuregui, C., Hodgson, J. G., and Field, K.: Leaf dry matter content is better at predicting above-ground net primary production than specific leaf area. Funct. Ecol., 31, 1336–1344, https://doi.org/10.1111/1365-2435.12832, 2017.

Telenius, A.: Biodiversity information goes public: GBIF at your service. Nord. J. Bot., 29, 378–381, https://doi.org/10.1111/j.1756-1051.2011.01167.x, 2011.

Thomas, D. S., Montagu, K. D., and Conroy, J. P.: Changes in wood density of *Eucalyptus camaldulensis* due to temperature-the physiological link between water viscosity and wood anatomy. Forest Ecol. Manag., 193, 157–165, https://doi.org/10.1016/j.foreco.2004.01.028, 2004.

Thomas, S. C.: Photosynthetic capacity peaks at intermediate size in temperate deciduous trees. Tree Physiol., 30, 555–573, https://doi.org/10.1093/treephys/tpq005, 2010.

Thuiller, W., Lafourcade, B., Engler, R., and Araújo, M. B.: BIOMOD – A platform for ensemble forecasting of species distributions. Ecography, 32, 369–373, https://doi.org/10.1111/j.1600-0587.2008.05742.x, 2009.

Trabucco, A., and Zomer, R. J.: Global Aridity Index and Potential Evapo-Transpiration (ET0) Climate Database v2. CGIAR Consortium for Spatial Information (CGIAR-CSI), https://cgiarcsi.community, 2018.

Vallicrosa, H., Sardans, J., Maspons, J., Zuccarini, P., Fernández-Martínez, M., Bauters, M., Goll, D. S., Ciais, P., Obersteiner, M., Janssens, I. A., and Peñuelas, J.: Global maps and factors driving forest foliar elemental composition: the importance of evolutionary history. New

Phytol., 233, 169–181, https://doi.org/10.1111/nph.17771, 2022.

van Bodegom, P. M., Douma, J. C., Witte, J. P. M., Ordoñez, J. C., Bartholomeus, R. P., and Aerts, R.: Going beyond limitations of plant functional types when predicting global ecosystem-atmosphere fluxes: exploring the merits of traits-based approaches. Global Ecol. Biogeogr., 21, 625–636, https://doi.org/10.1111/j.1466-8238.2011.00717.x, 2012.

van Bodegom, P. M., Douma, J. C., and Verheijen, L. M. A fully traits-based approach to modeling global vegetation distribution. P. Natl. Acad. Sci. USA, 111, 13733–13738, https://doi.org/10.1073/pnas.1304551110, 2014.

Verheijen, L. M., Aerts, R., Bonisch, G., Kattge, J., and van Bodegom, P. M.: Variation in trait trade-offs allows differentiation among predefined plant functional types: implications for predictive ecology. New Phytol., 209, 563–575, https://doi.org/10.1111/nph.13623, 2016.

Wang, H., Harrison, S. P., Prentice, I. C., Yang, Y. Z., Bai, F., Togashi, H. F., Wang, M., Zhou, S. X., and Ni, J.: The China Plant Trait Database: toward a comprehensive regional compilation of functional traits for land plants. Ecology, 99, 500, https://doi.org/10.1002/ecy.2091, 2018.

Webb, C. T., Hoeting, J. A., Ames, G. M., Pyne, M. I., and LeRoy Poff, N.: A structured and dynamic framework to advance traits-based theory and prediction in ecology. Ecol. Lett., 13, 267–283, https://doi.org/10.1111/j.1461-0248.2010.01444.x, 2010.

Wright, I. J., Dong, N., Maire, V., Prentice, I. C., Westoby, M., Diaz, S., Gallagher, R. V., Jacobs, B. F., Kooyman, R., Law, E. A., Leishman, M. R., Niinemets, U., Reich, P. B., Sack, L., Villar, R., Wang, H., and Wilf, P.: Global climatic drivers of leaf size. Science, 357, 917–921, https://doi.org/10.1126/science.aal4760, 2017.

Wright, I. J., Reich, P. B., Westoby, M., Ackerly, D. D., Baruch, Z., Bongers, F., Cavender-Bares, J., Chapin, T., Cornelissen, J. H. C., Diemer, M., Flexas, J., Garnier, E., Groom, P. K., Gulias, J., Hikosaka, K., Lamont, B. B., Lee, T., Lee, W., Lusk, C., Midgley, J. J., Navas, M. L., Niinemets, U., Oleksyn, J., Osada, N., Poorter, H., Poot, P., Prior, L., Pyankov, V. I., Roumet, C., Thomas, S. C., Tjoelker, M. G., Veneklaas, E. J., and Villar, R.: The worldwide leaf economics spectrum. Nature, 428, 821–827, https://doi.org/10.1038/nature02403, 2004.

Wullschleger, S. D., Epstein, H. E., Box, E. O., Euskirchen, E. S., Goswami, S., Iversen, C. M., Kattge, J., Norby, R. J., van Bodegom, P. M., and Xu, X.: Plant functional types in earth system models: past experiences and future directions for application of dynamic vegetation models in high-latitude ecosystems. Ann. Bot., 114, 1–16, https://doi.org/10.1093/aob/mcu077, 2014.

Yan, P., He, N. P., Yu, K. L., Xu, L., and Van Meerbeek, K.: Integrating multiple plant functional traits to predict ecosystem productivity. Commun. Biol., 6, 239, https://doi.org/10.1038/s42003-023-04626-3, 2023.

Yang, Y. Z., Zhu, Q. A., Peng, C. H., Wang, H., Xue, W., Lin, G. H., Wen, Z. M., Chang, J., Wang, M., Liu, G. B., and Li, S. Q.: A novel approach for modelling vegetation distributions and analysing vegetation sensitivity through trait-climate relationships in China. Sci. Rep., 6, 24110, https://doi.org/10.1038/srep24110, 2016.

Yang, Y. Z., Wang, H., Harrison, S. P., Prentice, I. C., Wright, I. J., Peng, C. H., and Lin, G. H.: Quantifying leaf-trait covariation and its controls across climates and biomes. New Phytol., 221, 155–168, https://doi.org/10.1111/nph.15422, 2018.

Yang, Y. Z., Zhao, J., Zhao, P. X., Wang, H., Wang, B. H., Su, S. F., Li, M. X., Wang, L. M., Zhu, Q. A., Pang, Z. Y., and Peng, C. H.: Trait-Based Climate Change Predictions of Vegetation Sensitivity and Distribution in China. Front. Plant Sci., 10, 908, https://doi.org/10.3389/fpls.2019.00908, 2019.

Yurova, A. Y., and Volodin, E. M.: Coupled simulation of climate and vegetation dynamics. Izv., Atmos. Ocean. Phy., 47, 531–539, https://doi.org/10.1134/s0001433811050124, 2011.

Zaehle, S., and Friend, A. D.: Carbon and nitrogen cycle dynamics in the O-CN land surface model: 1. Model description, site-scale evaluation, and sensitivity to parameter estimates. Global Biogeochem. Cy., 24, GB1005, https://doi.org/10.1029/2009gb003521, 2010.